Distributed Continual Learning with CoCoA in High-dimensional Linear Regression

Martin Hellkvist, Ayça Özçelikkale, Anders Ahlén

Abstract—We consider estimation under scenarios where the signals of interest exhibit change of characteristics over time. In particular, we consider the continual learning problem where different tasks, e.g., data with different distributions, arrive sequentially and the aim is to perform well on the newly arrived task without performance degradation on the previously seen tasks. In contrast to the continual learning literature focusing on the centralized setting, we investigate the problem from a distributed estimation perspective. We consider the well-established distributed learning algorithm CoCoA, which distributes the model parameters and the corresponding features over the network. We provide exact analytical characterization for the generalization error of CoCoA under continual learning for linear regression in a range of scenarios, where overparameterization is of particular interest. These analytical results characterize how the generalization error depends on the network structure, the task similarity and the number of tasks, and show how these dependencies are intertwined. In particular, our results show that the generalization error can be significantly reduced by adjusting the network size, where the most favorable network size depends on task similarity and the number of tasks. We present numerical results verifying the theoretical analysis and illustrate the continual learning performance of CoCoA with a digit classification task.

Index Terms—Multi-task networks, networked systems, distributed estimation, adaptation, overparametrization.

I. INTRODUCTION

When presented with a stream of data, continual learning [1], [2] is the act of learning from new data while not forgetting what was learnt previously. New data can, for instance, come from a related classification task with new fine-grained classes, or it can have statistical distribution shift compared to the previously seen data. Each set of data that is presented to the model is referred to as a *task*. Continual learning aims to create models which perform well on all seen tasks without the need to retrain from scratch when new data comes [1], [2]. Continual learning has been demonstrated for a large breadth of tasks with real world data, including image and gesture classification [3] and wireless system design [4], and has gained increasing attention during recent years [1]–[3], [5]–[8].

Continual learning is related to learning under non-stationary distributions and adaptive filtering, where iterative optimization methods and a stream of data are used to continuously adapt signal models to unknown and possibly changing environments [9]. Various phenomena of interest, such as financial time-series and target tracking, often exhibit structural changes in signal characteristics over time. Hence, performance under non-stationary distributions has been the focus in a number of scenarios; including randomly drifting unknowns in distributed learning [10], switching system dynamics [11]–[13].

The central issue in continual learning is *forgetting*, which measures the performance degradation on previously learned tasks as new tasks are learnt by the model [2], [5], [6]. If a model performs worse on the old tasks as new tasks are trained upon, the model is said to exhibit *catastrophic forgetting* [2], [5], [6]. This emphasis on the performance on old tasks is what distinguishes continual learning apart from the long line of existing work focusing on estimation with non-stationary distributions, where the estimator is expected to track the changing distribution, i.e., learn to perform well on the new distribution of data, but not necessarily on data from the previous distributions.

Significant effort has been put into studying continual learning empirically [14]–[17]. Compared to the breadth of existing empirical works, theoretical analysis of continual learning lacks behind. Nevertheless, bounds and explicit characterizations of continual learning performance have been recently presented for a range of models in order to close the gap between practice and theory, e.g., focusing on the least-squares estimator [18], the neural tangent regime [7], [8], and variants of stochastic gradient descent [5], [8], [18]. Here, we contribute to this line of work by considering the continual learning problem from a distributed learning perspective.

In distributed learning, optimization is performed over a network of computational nodes. It not only supports learning over large scale models by spreading the computational load over multiple computational units, such as in edge computing [19], but also provides an attractive framework for handling the emerging concerns for data security and privacy [20], [21]. Distributed learning is particularly attractive for scenarios where the data is already distributed over a network, e.g., in sensor networks [22]–[25], or in dictionary learning where sub-dictionaries are naturally separated over the network [26].

We focus on the successful distributed learning algorithm CoCoA [27]. CoCoA was developed from CoCoA-v1 [28] and CoCoA+ [29], and has been extended into the fully decentralized algorithm CoLA [30]. In CoCoA, nodes may utilize different local solvers with varying accuracies; allowing exploration of different communication and computation trade-offs [27]. Unlike the distributed learning frameworks where

The authors are with the Department of Electrical Engineering at Uppsala University, Uppsala, Sweden (e-mail: {Martin.Hellkvist, Ayca.Ozcelikkale, Anders.Ahlen}@angstrom.uu.se).

data samples, such as sensor readings, are distributed over the network [25]; in CoCoA, the unknown model parameters to be estimated and the corresponding features are distributed over the network, similar to [31], [32].

Our distributed continual learning framework with CoCoA is closely related to, but nevertheless different from, the typical framework for multitask learning over networks [33]–[35]. In particular, in our continual learning setting all nodes have the same task and this task changes over time for all nodes; whereas in typical settings for multitask learning over networks [33]–[35], the individual nodes have different tasks which do not change over time. Successful examples of continual learning over networks have been presented [36]–[38], under a range of constraints including asynchronous updates [38] and privacy [37]. In contrast to these works focusing on empirical performance, we focus on providing analytical performance guarantees for CoCoA.

We investigate how well CoCoA performs continual learning for a sequence of tasks where the data comes from a linear model for each task. We focus on the *generalization error* as our main performance metric. The generalization error measures the output prediction error that the model makes on all the tasks, using new data unseen during training, independent and identically distributed (i.i.d.) with the training data of the respective tasks. See Section II-C for a formal definition of the generalization error. We present closed form expressions of the generalization error for a range of scenarios under isotropic Gaussian regressors. **Our main contributions can be summarized as follows:**

- We provide exact analytical expressions for the generalization error of CoCoA under continual learning for the overparametrized case, as well as for the scenario with a single update for each task.
- We show that CoCoA can perform continual learning through both analytical characterization and numerical illustrations.
- Our analytical results characterize the dependence of the generalization error on the network structure as well as the number of tasks and the task similarity.
- We give sufficient conditions for a network structure to yield zero generalization error and training error for a large number of tasks under stationary data distributions.

Our work provides analytical characterizations of the generalization error, see, e.g., Theorem 1, Corollary 1, Theorem 2, Corollary 3 and Corollary 4, that have not been provided in the previous literature; and complement the numerical studies of continual learning with CoCoA in [39]. Our results extend the generalization error analysis in the single task setting of [40] to that of continual learning; and centralized continual learning setting of [18] to distributed learning. In contrast to [5] where the focus is on the training error for the case where the unknown model parameter vector is the same for all tasks, i.e., only the regressors change over the tasks, our analysis focuses on the generalization error when the tasks may possibly have different unknown model parameters.
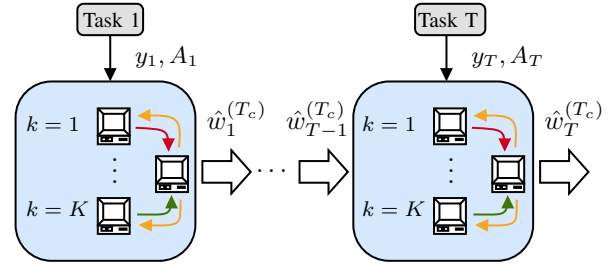
Fig. 1: Distributed continual learning with CoCoA, using T_c iterations, for a network of K nodes operating on T tasks.

Our closed form analytical expressions quantify the dependence of the generalization error to the number of samples per task, the number of nodes in the network, and the number of unknowns governed by each node as well as similarities between tasks. Here similarities between tasks are measured through inner products between model parameter vectors, see Theorem 1. We analytically quantify how the task similarity affects whether the error increases or decreases as the number of tasks increase. These results reveal that the generalization error can be significantly reduced by adjusting the network size where the most favorable network size depends on task similarity and the number of tasks. Furthermore, our numerical results illustrate that by reducing the number of CoCoA iterations for each task, one may obtain lower generalization error than if CoCoA is run until convergence; further illustrating that choosing CoCoA parameters that obtain the best continual learning performance is not straightforward.

The rest of the paper is organized as follows: Section II presents the problem formulation. Our characterization of the generalization error is provided in Section III together with a range of example scenarios. We illustrate our findings with numerical results in Section IV. Finally, we conclude the paper in Section VI.

Notation: Let $\boldsymbol{u}, \boldsymbol{q} \in \mathbb{R}^{d \times 1}$ be real-valued vectors. We denote the Euclidean norm as $\|\boldsymbol{u}\| = \sqrt{\langle \boldsymbol{u}, \boldsymbol{u} \rangle}$, where $\langle \boldsymbol{u}, \boldsymbol{q} \rangle = \boldsymbol{u}^\mathsf{T} \boldsymbol{q}$. We denote the weighted norm and inner product with $\|\boldsymbol{u}\|_{\boldsymbol{\Sigma}} = \sqrt{\langle \boldsymbol{u}, \boldsymbol{u} \rangle_{\boldsymbol{\Sigma}}}$, where $\langle \boldsymbol{u}, \boldsymbol{q} \rangle_{\boldsymbol{\Sigma}} = \boldsymbol{u}^\mathsf{T} \boldsymbol{\Sigma} \boldsymbol{q}$ for any symmetric positive semi-definite matrix $\boldsymbol{\Sigma} \in \mathbb{R}^{d \times d}$. The Moore-Penrose pseudoinverse and transpose of a matrix $\boldsymbol{A}$ are denoted by $\boldsymbol{A}^+$ and $\boldsymbol{A}^\mathsf{T}$, respectively. The $p \times p$ identity matrix is denoted as $\boldsymbol{I}_p$. The notation $\boldsymbol{u} \sim \mathcal{N}(\boldsymbol{\mu}, \boldsymbol{\Sigma})$ denotes that $\boldsymbol{u} \in \mathbb{R}^{d \times 1}$ is a Gaussian random vector with the mean $\boldsymbol{\mu} \in \mathbb{R}^{d \times 1}$ and the covariance matrix $\boldsymbol{\Sigma} \in \mathbb{R}^{d \times d}$. For a vector of unknown parameters $\boldsymbol{w}^* \in \mathbb{R}^{p \times 1}$, the superscript * is used to emphasize that this is the true value of the unknown vector. For products where the lower limit exceeds the upper limit, we use the convention $\prod_{\ell=\tau}^{\tau-1} \boldsymbol{M}_\ell = \boldsymbol{I}_p$, where $\boldsymbol{M}_\ell \in \mathbb{R}^{p \times p}$ are non-zero matrices.

II. PROBLEM STATEMENT

A. Definition of a Task

We consider the continual learning problem of solving T tasks. The *training data* for task t, $1 \leq t \leq T$ is denoted by $(\boldsymbol{y}_t, \boldsymbol{A}_t)$ and consists of the regressor matrix $\boldsymbol{A}_t \in \mathbb{R}^{n_t \times p}$

and the corresponding vector of outputs $\boldsymbol{y}_t \in \mathbb{R}^{n_t \times 1}$. The observations $\boldsymbol{y}_t$ come from the following noisy linear model

$$\boldsymbol{y}_t = \boldsymbol{A}_t \boldsymbol{w}_t^* + \boldsymbol{z}_t. \tag{1}$$

where each task has an unknown model parameter vector $\boldsymbol{w}_t^* \in \mathbb{R}^{p \times 1}$, and $\boldsymbol{z}_t \in \mathbb{R}^{n_t \times 1}$ denotes the noise. The noise vectors $\boldsymbol{z}_t$'s are independently distributed with $\boldsymbol{z}_t \sim \mathcal{N}(\boldsymbol{0}, \sigma_t^2 \boldsymbol{I}_{n_t})$, and they are statistically independent from the regressors. We focus on the following regressor model:

Assumption 1. *The matrices $\boldsymbol{A}_t$, $t = 1, \ldots, T$, are statistically independent and have independently and identically distributed (i.i.d.) standard Gaussian entries. In particular, if $\boldsymbol{a}^\intercal \in \mathbb{R}^{1 \times p}$ is a row of $\boldsymbol{A}_t$, then $\boldsymbol{a} \sim \mathcal{N}(\boldsymbol{0}, \boldsymbol{I}_p)$.*

Task t corresponds to finding an estimate $\hat{\boldsymbol{w}}$ so that $\boldsymbol{y}_t \approx \boldsymbol{A}_t \hat{\boldsymbol{w}}$. In particular, for task t, the aim is to minimize the training error given by the mean-squared-error (MSE)

$$\ell_t(\hat{\boldsymbol{w}}) = \frac{1}{2n_t} \left\| \boldsymbol{A}_t \hat{\boldsymbol{w}} - \boldsymbol{y}_t \right\|^2, \tag{2}$$

where $\| \cdot \|$ denotes the Euclidean norm. Note that the scaling of $\frac{1}{2}$ is included here for notational convenience later.

B. Continual Learning Problem

We study the continual learning setting, where training data for the tasks arrive sequentially, and the data for only one task is available at a given time. In particular, at a given time instant t, we only have access to $(\boldsymbol{y}_t, \boldsymbol{A}_t)$ for a particular task t but not the data for the other tasks. The goal is to find an estimate $\hat{\boldsymbol{w}}$ that performs well over all tasks $1 \leq t \leq T$. Hence, we would like to find a single $\hat{\boldsymbol{w}}$ such that

$$\boldsymbol{A}_t \hat{\boldsymbol{w}} \approx \boldsymbol{y}_t, \ \forall t. \tag{3}$$

We note that if all the data were available at once, instead of arriving sequentially, one may find a solution for (3) by solving the minimization problem $\min_{\boldsymbol{w}} \frac{1}{2N} \sum_{t=1}^{T} \| \boldsymbol{A}_t \boldsymbol{w} - \boldsymbol{y}_t \|^2$, where $N = \sum_{t=1}^{T} n_t$. Hence, the aim of the continual learning setting can be seen as to perform as close as possible to this solution, despite the sequential nature of data arrival. Further details on this benchmark can be found in Section II-E.

We focus on the scenarios where the task identity, i.e., t, is not available and it does not need to be inferred; hence we look for a single $\hat{\boldsymbol{w}}$ for all tasks. This type of continual setting is referred as domain-incremental learning; and it is suited to the scenarios where the structure of the tasks is the same but the input distribution changes [41].

Precise definitions of the performance metrics for continual learning are presented in Section II-C. We provide a detailed description of the distributed iterative algorithm CoCoA employed to find the estimate in Section II-D, see also Fig. 1. An overview of some of the important variables of the problem formulation is provided in Table I.

C. Performance Metrics

Let $\hat{\boldsymbol{w}}_\tau$ denote an estimate obtained by training on a dataset $\mathcal{D}_\tau = \{\boldsymbol{y}_t, \boldsymbol{A}_t\}_{t=1}^{\tau}$ where $1 \leq \tau \leq T$. Note that the subscript τ of the estimate $\hat{\boldsymbol{w}}_\tau$ indicates that the data up to and including task τ has been used to create the estimate.

TABLE I: Overview of Important Variables.

$\boldsymbol{w}_t^*$	true value of the unknown parameter for task t
$(\boldsymbol{y}_t, \boldsymbol{A}_t)$	training data for task t
$\mathcal{D}_t$	$\{\boldsymbol{y}_{t'}, \boldsymbol{A}_{t'}\}_{t'=1}^{t}$
$\hat{\boldsymbol{w}}_t$	parameter estimate found using $\mathcal{D}_t$
$\hat{\boldsymbol{w}}_t^{(i)}$	parameter estimate found by CoCoA using $\mathcal{D}_t$ and i iterations for task t
$\hat{\boldsymbol{w}}_{t,[k]}^{(i)}$	partition of $\hat{\boldsymbol{w}}_t^{(i)}$ at node k of the network

To characterize how well an estimate achieves continual learning, we consider forgetting from two different perspectives: *training error* and *generalization error*.

1) Training Error: Forgetting in terms of training error measures the output error that an estimate makes on the training data of the tasks previously seen. It is defined as [5]

$$f_\tau(\hat{\boldsymbol{w}}_\tau) = \frac{1}{\tau} \sum_{t=1}^{\tau} \ell_t(\hat{\boldsymbol{w}}_\tau) = \frac{1}{\tau} \sum_{t=1}^{\tau} \frac{1}{2n_t} \left\| \boldsymbol{A}_t \hat{\boldsymbol{w}}_\tau - \boldsymbol{y}_t \right\|^2. \tag{4}$$

Hence, $f_\tau(\hat{\boldsymbol{w}}_\tau)$ is the average MSE over the training data used to create the estimate $\hat{\boldsymbol{w}}_\tau$, i.e., from the tasks $t = 1, \ldots, \tau$.

We define the *expected training error* of $\hat{\boldsymbol{w}}_\tau$ over the distribution of the training data $\mathcal{D}_\tau$ as

$$F_\tau(\hat{\boldsymbol{w}}_\tau) = \underset{\mathcal{D}_\tau}{\mathbb{E}} \left[f_\tau(\hat{\boldsymbol{w}}_\tau) \right] \tag{5}$$

$$= \frac{1}{\tau} \sum_{t=1}^{\tau} \frac{1}{2n_t} \underset{\mathcal{D}_\tau}{\mathbb{E}} \left[\left\| \boldsymbol{A}_t \hat{\boldsymbol{w}}_\tau - \boldsymbol{y}_t \right\|^2 \right]. \tag{6}$$

Since $\hat{\boldsymbol{w}}_\tau$ depends on data up to and including task τ, the expectation in (6) is over $\mathcal{D}_\tau = \{\boldsymbol{y}_t, \boldsymbol{A}_t\}_{t=1}^{\tau}$ and not merely over only the latest task $(\boldsymbol{y}_\tau, \boldsymbol{A}_\tau)$.

2) Generalization Error: The generalization error measures the performance on data unseen during training. Let $y_{t,\text{new}} = \boldsymbol{a}_{t,\text{new}}^\intercal \boldsymbol{w}_t^* + z_{t,\text{new}}$, be a new unseen sample for task t, i.i.d. with the samples of training data of that task, i.e., $\boldsymbol{a}_{t,\text{new}} \sim \mathcal{N}(\boldsymbol{0}, \boldsymbol{I}_p)$ and $z_{t,\text{new}} \sim \mathcal{N}(0, \sigma_t^2)$. Consider the estimate $\hat{\boldsymbol{w}}_\tau$. The generalization error associated with $\hat{\boldsymbol{w}}_\tau$ over tasks $t = 1, \ldots, T$, is defined as

$$g_T(\hat{\boldsymbol{w}}_\tau) = \frac{1}{T} \sum_{t=1}^{T} \underset{y_{t,\text{new}}, \boldsymbol{a}_{t,\text{new}}}{\mathbb{E}} \left[\left(\boldsymbol{a}_{t,\text{new}}^\intercal \hat{\boldsymbol{w}}_\tau - y_{t,\text{new}} \right)^2 \right] \tag{7}$$

$$= \frac{1}{T} \sum_{t=1}^{T} \underset{\boldsymbol{a}_{t,\text{new}}, z_{t,\text{new}}}{\mathbb{E}} \left[\left(\boldsymbol{a}_{t,\text{new}}^\intercal (\hat{\boldsymbol{w}}_\tau - \boldsymbol{w}_t^*) - z_{t,\text{new}} \right)^2 \right] \tag{8}$$

$$= \frac{1}{T} \sum_{t=1}^{T} (\hat{\boldsymbol{w}}_\tau - \boldsymbol{w}_t^*)^\intercal \underset{\boldsymbol{a}_{t,\text{new}}}{\mathbb{E}} \left[\boldsymbol{a}_{t,\text{new}} \boldsymbol{a}_{t,\text{new}}^\intercal \right] (\hat{\boldsymbol{w}}_\tau - \boldsymbol{w}_t^*) + \underset{z_{t,\text{new}}}{\mathbb{E}} \left[z_{t,\text{new}}^2 \right] \tag{9}$$

$$= \frac{1}{T} \sum_{t=1}^{T} \left\| \hat{\boldsymbol{w}}_\tau - \boldsymbol{w}_t^* \right\|^2 + \sigma_t^2. \tag{10}$$

Forgetting is typically defined only on the tasks whose data is used for constructing the estimate [2], [5], see for instance the summation in (4) which runs up to τ. On the other hand, here we have chosen to define the generalization error in (10) as the performance over all tasks $1 \leq t \leq T$ instead of only up to the last seen task τ. In addition to measuring the forgetting

---
Algorithm 1: COCOA for task t

---
1 **Input**: Training data $\left(\boldsymbol{y}_t, \boldsymbol{A}_t = [\boldsymbol{A}_{t,[1]}, \ldots, \boldsymbol{A}_{t,[K]}]\right)$,
  previous estimate $\hat{\boldsymbol{w}}_{t-1}^{(T_c)}$, number of iterations T_c for
  COCOA to run per task.
2 **Initialize:** $\hat{\boldsymbol{w}}_t^{(0)} = \hat{\boldsymbol{w}}_{t-1}^{(T_c)}$,
3 $\boldsymbol{v}_{t,[k]}^{(0)} = K\boldsymbol{A}_{t,[k]}\hat{\boldsymbol{w}}_{t,[k]}^{(0)}$, $k = 1, \ldots, K$.
4 **for** $i = 1, \ldots, T_c$ **do**
5    $\bar{\boldsymbol{v}}_t^{(i)} = \frac{1}{K}\sum_{k=1}^{K}\boldsymbol{v}_{t,[k]}^{(i-1)}$
6   **for** $k \in \{1, 2, \ldots, K\}$ **do**
7       $\Delta\hat{\boldsymbol{w}}_{t,[k]}^{(i)} = \frac{1}{K}\boldsymbol{A}_{t,[k]}^{+}\left(\boldsymbol{y}_t - \bar{\boldsymbol{v}}_t^{(i)}\right)$
8       $\hat{\boldsymbol{w}}_{t,[k]}^{(i)} = \hat{\boldsymbol{w}}_{t,[k]}^{(i-1)} + \Delta\hat{\boldsymbol{w}}_{t,[k]}^{(i)}$
9       $\boldsymbol{v}_{t,[k]}^{(i)} = \bar{\boldsymbol{v}}_t^{(i)} + K\boldsymbol{A}_{t,[k]}\Delta\hat{\boldsymbol{w}}_{t,[k]}^{(i)}$

10 **Output:** $\hat{\boldsymbol{w}}_t^{(T_c)}$

---

in terms of generalization on the tasks seen, this definition allows us to keep track of how well the estimate performs for unseen tasks and leads to interesting conclusions in terms of effect of task similarity, see Remark 2.

We define the *expected generalization error* over the distribution of the training data $\mathcal{D}_\tau$ as

$$G_T(\hat{\boldsymbol{w}}_\tau) = \mathop{\mathbb{E}}_{\mathcal{D}_\tau}\left[g_T(\hat{\boldsymbol{w}}_\tau)\right] \tag{11}$$

$$= \frac{1}{T}\sum_{t=1}^{T}\mathop{\mathbb{E}}_{\mathcal{D}_\tau}\left[\|\hat{\boldsymbol{w}}_\tau - \boldsymbol{w}_t^*\|^2\right] + \sigma_t^2. \tag{12}$$

Our main results in Theorem 1 provide an analytical characterization of $G_T(\cdot)$ when the estimate $\hat{\boldsymbol{w}}_\tau$ is obtained using the distributed algorithm COCOA.

D. Distributed Continual Learning with COCOA

1) Overview: Consider task t with data $(\boldsymbol{y}_t, \boldsymbol{A}_t)$. We minimize the MSE in (2) in a distributed and iterative fashion using the algorithm COCOA [27], see Figure 1 and Algorithm 1. For task t, the regressor matrix $\boldsymbol{A}_t$ and the initial estimate for the unknown vector is distributed over K nodes. Then, T_c iterations of COCOA are used to update the parameter estimate iteratively in order to minimize (2). When a new task comes, the old parameter estimate is used as the initialization and the procedure is repeated. The below presentation of COCOA includes references to the line numbers in Algorithm 1.

2) Distribution over nodes: We now describe how the data is distributed over the network. The regressor matrix $\boldsymbol{A}_t$ is distributed over a network of K nodes by column-wise partitions such that each node governs an exclusive set of columns of $\boldsymbol{A}_t$. The partitioning of $\boldsymbol{A}_t$ is given by

$$\boldsymbol{A}_t = \begin{bmatrix} \boldsymbol{A}_{t,[1]} & \cdots & \boldsymbol{A}_{t,[K]} \end{bmatrix}. \tag{13}$$

We have $\boldsymbol{A}_{t,[k]} \in \mathbb{R}^{n_t \times p_k}$, $\forall t$, hence the number of columns in the kth submatrix of $\boldsymbol{A}_t$ is $p_k \in \mathbb{N}$, $\forall t$.

Let us denote the model parameter estimate obtained after training on the data of task t with i iterations of COCOA by

$\hat{\boldsymbol{w}}_t^{(i)} \in \mathbb{R}^{p \times 1}$. The column-wise partitioning of $\boldsymbol{A}_t$ corresponds to a row-wise partitioning in $\hat{\boldsymbol{w}}_t^{(i)}$ over the nodes as follows

$$\hat{\boldsymbol{w}}_t^{(i)} = \begin{bmatrix} \hat{\boldsymbol{w}}_{t,[1]}^{(i)} \\ \vdots \\ \hat{\boldsymbol{w}}_{t,[K]}^{(i)} \end{bmatrix}, \tag{14}$$

where $\hat{\boldsymbol{w}}_{t,[k]}^{(i)} \in \mathbb{R}^{p_k \times 1}$ is the unknown model parameter partition at node k.

3) Learning over tasks: Let us have task $t - 1$. We run COCOA for T_c iterations to obtain the estimate $\hat{\boldsymbol{w}}_{t-1}^{(T_c)}$. When data for task t comes, i.e., $(\boldsymbol{y}_t, \boldsymbol{A}_t)$, the algorithm is initialized with the estimate learnt with the data of the previous task, i.e.,

$$\hat{\boldsymbol{w}}_t^{(0)} = \hat{\boldsymbol{w}}_{t-1}^{(T_c)}, \tag{15}$$

see line 2. For the first task, i.e. $t = 1$, we use $\hat{\boldsymbol{w}}_1^{(0)} = \hat{\boldsymbol{w}}_0^{(T_c)} = \boldsymbol{0}$ as initialization. In COCOA, an auxiliary variable $\boldsymbol{v}_t$ keeps track of the contribution of each node to the current estimate of the observations $\boldsymbol{y}_t$. Partitions of $\boldsymbol{v}_t$ are initialized as

$$\boldsymbol{v}_{t,[k]}^{(0)} = K\boldsymbol{A}_{t,[k]}\hat{\boldsymbol{w}}_{t,[k]}^{(0)}, \quad \forall k, \tag{16}$$

see line 3. After T_c iterations of COCOA for task t, $\hat{\boldsymbol{w}}_t^{(T_c)}$ is outputted as the estimate of the parameter vector, see line 10.

4) COCOA iterations: For each iteration (i), a central unit shares the network's aggregated current estimate of the observations $\boldsymbol{y}_t$, denoted by $\bar{\boldsymbol{v}}_t^{(i)} \in \mathbb{R}^{n_t \times 1}$ (line 5). Each node then computes its local updates $\Delta\hat{\boldsymbol{w}}_{t,[k]}^{(i)} \in \mathbb{R}^{p_k \times 1}$ (line 7), updates its estimate of the parameter partition $\hat{\boldsymbol{w}}_{t,[k]}^{(i)}$ (line 8) and the local estimate of $\boldsymbol{y}$, i.e., $\boldsymbol{v}_{t,[k]}^{(i)} \in \mathbb{R}^{n_t \times 1}$ (line 9).

In order to minimize (2), the node k's update in line 7 is computed by solving the following local subproblem [27]

$$\min_{\Delta\hat{\boldsymbol{w}}_{t,[k]}^{(i)}} \frac{1}{2Kn_t}\left\|\bar{\boldsymbol{v}}_t^{(i)} - \boldsymbol{y}_t\right\|^2 + \frac{\sigma'}{2n_t}\left\|\boldsymbol{A}_{t,[k]}\Delta\hat{\boldsymbol{w}}_{t,[k]}^{(i)}\right\|^2$$
$$+ \frac{1}{n_t}\left(\bar{\boldsymbol{v}}_t^{(i)} - \boldsymbol{y}_t\right)^{\mathsf{T}}\boldsymbol{A}_{t,[k]}\Delta\hat{\boldsymbol{w}}_{t,[k]}^{(i)}. \tag{17}$$

This is a convex problem in $\Delta\hat{\boldsymbol{w}}_{t,[k]}^{(i)}$. Setting its derivative with respect to $\Delta\hat{\boldsymbol{w}}_{t,[k]}^{(i)}$ to zero, one arrives at the following

$$\sigma'\boldsymbol{A}_{t,[k]}^{\mathsf{T}}\boldsymbol{A}_{t,[k]}\Delta\hat{\boldsymbol{w}}_{t,[k]}^{(i)} = \boldsymbol{A}_{t,[k]}^{\mathsf{T}}\left(\boldsymbol{y}_t - \bar{\boldsymbol{v}}_t^{(i)}\right). \tag{18}$$

The expression in line 7 is the minimum ℓ_2-norm solution to (18) where $(\cdot)^+$ in line 7 denotes the Moore-Penrose pseudoinverse.

In [27], COCOA is presented with the hyperparameters σ' and $\bar{\varphi}$, referred to as the subproblem and aggregation parameters, respectively. We have set $\sigma' = \bar{\varphi}K$, and let $\bar{\varphi} \in (0, 1]$, as these are considered safe choices [30]. As a result, the specific value of $\bar{\varphi}$ washes out to give the explicit expressions in Algorithm 1.

E. A benchmark: Offline and centralized solution

We compare the performance of the COCOA solution with the following offline and centralized version of the problem. In particular, consider the setting where one has access to all the tasks' training data at once, hence one minimizes MSE over all

that data simultaneously, i.e., $\min_{\boldsymbol{w}} \frac{1}{2N} \sum_{t=1}^{T} \|\boldsymbol{A}_t \boldsymbol{w} - \boldsymbol{y}_t\|^2$, where $N = \sum_{t=1}^{T} n_t$. The minimum ℓ_2-norm solution, i.e., the standard least-squares solution, is then given by,

$$\hat{\boldsymbol{w}}_{\text{LS}} = \begin{bmatrix} \boldsymbol{A}_1 \\ \vdots \\ \boldsymbol{A}_T \end{bmatrix}^{+} \begin{bmatrix} \boldsymbol{y}_1 \\ \vdots \\ \boldsymbol{y}_{T\cdot} \end{bmatrix}. \tag{19}$$

We refer to $\hat{\boldsymbol{w}}_{\text{LS}}$ as the *offline and centralized solution*, and we use it to compare the performance of CoCoA with.

III. GENERALIZATION ERROR

In this section, we present closed form expressions for the generalization error of the estimates produced by Algorithm 1 in the continual learning setting for a range of scenarios.

A. Preliminaries

We begin by presenting Lemma 1, which describes the estimate $\hat{\boldsymbol{w}}_t^{(1)}$, i.e., the estimate found by Algorithm 1 after the first iteration when initialized with the parameter estimate from the previous task, i.e., $\hat{\boldsymbol{w}}_{t-1}^{(T_c)}$. Note that Lemma 1 and also some other intermediate results, such as Lemma 5, do not rely on Assumption 1. Hence, for the sake of clarity, we refer to Assumption 1 in our results explicitly whenever it is needed.

Lemma 1. *The solution $\hat{\boldsymbol{w}}_t^{(1)}$ after first iteration of Algorithm 1 is given by the following expression,*

$$\hat{\boldsymbol{w}}_t^{(1)} = \boldsymbol{P}_t \hat{\boldsymbol{w}}_{t-1}^{(T_c)} + \bar{\boldsymbol{A}}_t \boldsymbol{y}_t, \tag{20}$$

where

$$\boldsymbol{P}_t = \boldsymbol{I}_p - \bar{\boldsymbol{A}}_t \boldsymbol{A}_t \in \mathbb{R}^{p \times p}, \tag{21}$$

$$\bar{\boldsymbol{A}}_t = \frac{1}{K} \begin{bmatrix} \boldsymbol{A}_{t,[1]}^{+} \\ \vdots \\ \boldsymbol{A}_{t,[K]}^{+} \end{bmatrix} \in \mathbb{R}^{p \times n_t}. \tag{22}$$

Furthermore, for any $\boldsymbol{u} \in \mathbb{R}^{p \times 1}$,

$$\hat{\boldsymbol{w}}_t^{(1)} - \boldsymbol{u} = \boldsymbol{P}_t \left(\hat{\boldsymbol{w}}_{t-1}^{(T_c)} - \boldsymbol{u} \right) + \bar{\boldsymbol{A}}_t \boldsymbol{A}_t (\boldsymbol{w}_t^* - \boldsymbol{u}) + \bar{\boldsymbol{A}}_t \boldsymbol{z}_t. \tag{23}$$

Proof: This result has been partially presented in [39, Sec. 3], [40, Sec. IV]. Due to slightly different assumptions therein, we present the proof in Appendix B for the sake of completeness.

The recursion in (23) is used to present closed form expressions of the generalization error in Theorem 1, and asymptotic analyses of the generalization and training error in Section III-E. The following result gives a sufficient condition for which the algorithm converges in the first iteration.

Lemma 2. *If the partitions $\boldsymbol{A}_{t,[k]} \in \mathbb{R}^{n_t \times p_k}$ have full row rank, i.e., $Rank(\boldsymbol{A}_{t,[k]}) = n_t$, then Algorithm 1 converges in the first iteration to the solution given by (20) i.e.,*

$$\hat{\boldsymbol{w}}_t^{(T_c)} = \hat{\boldsymbol{w}}_t^{(1)}, \ T_c \geq 1. \tag{24}$$

Proof: This result is proven in [39, Lemma 1]. Note that the first half of [39, Lemma 1], i.e., the result here, does not require the stationarity condition [39, Assumption 1].

We use one of the following assumptions in most of our analytical development:

Assumption 2. $p_k > n_t + 1, \ \forall t, k.$

Assumption 3. $T_c = 1.$

We explicitly refer to these assumptions in our results as appropriate.

Recall that for a given task t, all nodes have the same number of data samples n_t but possibly different number of model parameters. Assumption 2 corresponds to the case of overparameterized local models, i.e., at each node k there is a large number of model parameters p_k compared to the number of data samples n_t. Many modern learning models operate in the overparameterized regime [42], and massively overparametrized models have been very successful, see for instance [42, Table 1]. A number of works have focused on the overparametrized setting under distributed learning, investigating theoretical guarantees for communication efficiency [43]–[45], convergence [46], [47] and generalization error [40]. In addition to the empirical success of large overparametrized models [42, Table 1], analytical characterization of the generalization error of overparametrized linear models has also been the focus of many recent works, including the centralized scenario, e.g. [48]–[50], and distributed scenario without continual learning [40]. In this article, we contribute to these lines of work by focusing on a distributed and continual learning setting.

Assumption 3 corresponds to the setting that only one update to the parameter estimate is performed for a given task, i.e., there is one round of communication between the nodes. Our work here can be interpreted as the generalization of the centralized continual learning scenario in [18], which also performs a one step update, to the distributed case. See Section III-D for further discussions. In distributed learning, the scenarios with one round of communication, is referred to as the one-shot setting [51]–[53]. In practice, this type of setting may be used when the cost of communication is too high; or when the computational memory load and the related energy constraints make it difficult for the nodes to perform multiple updates; or when the data comes in real-time and it cannot be stored for the subsequent updates due to memory constraints. Distributed one-shot settings have been the main focus of a number of works, such as [52]–[55]. For some scenarios, one-shot solutions have been shown to outperform or match standard solutions, including the mixture weight method, which uses one-shot communication and less resources overall while achieving a performance on the level of the standard gradient-based approach with multiple rounds of communication [56]; approaches based on averaging, which use one-shot communication but achieve the best possible error rate decay achievable by a centralized algorithm [57]; and one-shot averaging with stochastic gradient, which can achieve the optimal asymptotic convergence rate [58]. In a similar manner, running CoCoA with $T_c = 1$ can in some scenarios provide better generalization performance compared to having a relatively high T_c, see the discussion for high number of

tasks in Section IV-D.

Remark 1. *If Assumption 1 and Assumption 2 hold, then the partitions $\boldsymbol{A}_{t,[k]}$ are full row-rank with probability 1, hence (24) holds with probability 1. As a result, the expected generalization error $G_T(\hat{\boldsymbol{w}}_t^{(T_c)})$ given by Algorithm 1 with $T_c = 1$ is the same for all $T_c \geq 1$.*

The results presented in this paper are often functions of the problem dimensions. In particular, the dimensions of the local partitions $\boldsymbol{A}_{t,[k]} \in \mathbb{R}^{n_t \times p_k}$, i.e., the number of samples per task n_t, and the number of model parameters per node p_k. Thus we introduce the following notation for the nodes $k = 1, \ldots, K$, and the tasks $t = 1, \ldots, T$,

$$r_{t,k} = \frac{\min(n_t, p_k)}{p_k}, \tag{25}$$

$$\gamma_{t,k} = \begin{cases} \dfrac{\min(n_t, p_k)}{\max(n_t, p_k) - \min(n_t, p_k) - 1}, & p_k \notin [n_t \pm 1] \tag{26a} \\ +\infty, & \text{otherwise.} \tag{26b} \end{cases}$$

where the notation $[n_t \pm 1]$ represents the range $[n_t - 1, n_t + 1]$. Note that the infinity, i.e., ∞, is a short-hand notation for indeterminate/infinite values in the expressions.

B. Generalization Error

We now present our main result:

Theorem 1. *Let Assumption 1 hold, and the noise vectors be independently distributed as $\boldsymbol{z}_j \sim \mathcal{N}(\boldsymbol{0}, \sigma_j^2 \boldsymbol{I}_{n_j})$, and independent of the regressors. Let Assumption 2 or 3 hold. Then, over the distribution of $\hat{\boldsymbol{w}}_t^{(T_c)}$ as a function of the training data $\mathcal{D}_t = \{(\boldsymbol{y}_j, \boldsymbol{A}_j)\}_{j=1}^t$, we have the expected generalization error in (12) as,*

$$G_T(\hat{\boldsymbol{w}}_t^{(T_c)}) = \frac{1}{T} \sum_{i=1}^T \|\boldsymbol{w}_i^*\|_{\boldsymbol{H}_1^{\{t\}}}^2 + \phi\left(\hat{\boldsymbol{w}}_t^{(T_c)}, \boldsymbol{w}_i^*\right) + \sigma_i^2 \tag{27}$$

where $\boldsymbol{w}_i^*$ denote the model unknowns in (1), and where

$$\phi\left(\hat{\boldsymbol{w}}_t^{(T_c)}, \boldsymbol{w}_i^*\right) = \sum_{\tau=1}^t \left(\|\boldsymbol{w}_\tau^* - \boldsymbol{w}_i^*\|_{\boldsymbol{R}_\tau^{\{t\}}}^2 + \sigma_\tau^2 \frac{\sum_{k=1}^K \gamma_{\tau,k} h_{\tau+1,k}}{K^2} \right.$$
$$\left. + 2 \sum_{j=0}^{\tau-1} \langle \boldsymbol{w}_\tau^* - \boldsymbol{w}_i^*, \boldsymbol{w}_j^* - \boldsymbol{w}_i^* \rangle_{\boldsymbol{Q}_{\tau,j}^{\{t\}}} \right), \tag{28}$$

with $\gamma_{t,k}$ defined as in (26), and where $\boldsymbol{w}_0^* = \boldsymbol{0}$,

$$\boldsymbol{H}_1^{\{t\}} = diag\{h_{1,k} \boldsymbol{I}_{p_k}\}_{k=1}^K \tag{29}$$

$$\boldsymbol{R}_\tau^{\{t\}} = diag\left\{ \frac{h_{\tau+1,k} r_{\tau,k} + \sum_{\substack{i=1 \\ i \neq k}}^K h_{\tau+1,i} \gamma_{\tau,i}}{K^2} \boldsymbol{I}_{p_k} \right\}_{k=1}^K, \tag{30}$$

$$\boldsymbol{Q}_{\tau,j}^{\{t\}} = diag\left\{ \frac{r_{j,k}}{K} \prod_{\ell=j+1}^{\tau-1} \left(1 - \frac{r_{\ell,k}}{K}\right) \right. \tag{31}$$
$$\left. \times \frac{h_{\tau+1,k} r_{\tau,k}(K-1) - \sum_{\substack{i=1 \\ i \neq k}}^K h_{\tau+1,i} \gamma_{\tau,i}}{K^2} \boldsymbol{I}_{p_k} \right\}_{k=1}^K, \tag{32}$$

for $\tau = 1, \ldots, t$, and where $r_{t,k}$ is defined as in (25), with $r_{0,k} = K$, and where

$$h_{\tau,k} = \frac{h_{\tau+1,k}\left(K^2 + r_{\tau,k}(1-2K)\right) + \sum_{\substack{i=1 \\ i \neq k}}^K h_{\tau+1,i} \gamma_{\tau,i}}{K^2}, \tag{33}$$

for $\tau = 1, \ldots, t$, and where $h_{t+1,k} = 1$, $k = 1, \ldots, K$.

Proof: See Appendix C.

Theorem 1 provides closed form expressions for the generalization error for a stream of incoming tasks as a function of the noise levels σ_i^2, the number of samples per task n_i, the number of nodes in the network, K, and the number of unknowns governed by each node, p_k, as well as similarities between tasks through $\|\boldsymbol{w}_\tau^* - \boldsymbol{w}_i^*\|^2$ and $\langle \boldsymbol{w}_\tau^* - \boldsymbol{w}_i^*, \boldsymbol{w}_j^* - \boldsymbol{w}_i^* \rangle$.

Remark 2. *For generality, we have used $\hat{\boldsymbol{w}}_t^{(T_c)}$ where the estimate is trained on the first t tasks, rather than $\hat{\boldsymbol{w}}_T^{(T_c)}$ which is trained on all the T tasks. As a result, the cross-terms $\|\boldsymbol{w}_\tau^* - \boldsymbol{w}_i^*\|^2$ and $\langle \boldsymbol{w}_\tau^* - \boldsymbol{w}_i^*, \boldsymbol{w}_j^* - \boldsymbol{w}_i^* \rangle$, i.e., the direct effect of task similarity, are only present for $\tau \leq t$ and $j < \tau$.*

Remark 3. *If $p_k \in [n_t \pm 1]$, then the local sub-problems in the nodes become ill-conditioned with high-probability and the generalization error of* COCOA *diverges. See [40] for detailed discussions.*

Theorem 1 shows that the network structure can have a large effect on the generalization error. This effect goes beyond what has been described in Remark 3. For instance, whether the error increases with the increasing number of tasks depends on the number of nodes in the network. The task similarity also heavily influences whether the error increases or decreases as the number of tasks increases. We further discuss these effects in Section IV-B.

C. Special Case of Equal Dimensions

We now consider the special case where the problem dimensions are the same for all tasks and at all nodes:

Corollary 1. *Consider the setting of Theorem 1 in the special case that all tasks have the same number of samples, i.e., $n_t = n$, $\forall t$, and all nodes have the same number of unknowns, and $p_k = \frac{p}{K}$, $\forall k$. With $r = r_{t,k}$ and $\gamma = \gamma_{t,k}$ as in (25) – (26), we then have*

$$G_T\left(\hat{\boldsymbol{w}}_t^{(T_c)}\right) = \frac{1}{T} \sum_{i=1}^T \left[\|\boldsymbol{w}_i^*\|^2 h^t + \sigma_i^2 \right.$$
$$+ \sum_{\tau=1}^t \left(\|\boldsymbol{w}_\tau^* - \boldsymbol{w}_i^*\|^2 \frac{r + (K-1)\gamma}{K^2} h^{t-\tau} + \sigma_\tau^2 \frac{\gamma}{K} h^{t-\tau} \right.$$
$$+ 2 h^{t-\tau}(r - \gamma) \frac{K-1}{K^2} \frac{r}{K} \sum_{j=1}^{\tau-1} \left(1 - \frac{r}{K}\right)^{\tau-j-1} \tag{34}$$
$$\times \langle \boldsymbol{w}_\tau^* - \boldsymbol{w}_i^*, \boldsymbol{w}_j^* - \boldsymbol{w}_i^* \rangle$$
$$\left. - 2\frac{K-1}{K^2} \left(1 - \frac{r}{K}\right)^{\tau-1}(r - \gamma) h^{t-\tau} \langle \boldsymbol{w}_\tau^* - \boldsymbol{w}_i^*, \boldsymbol{w}_i^* \rangle \right) \Bigg],$$

with

$$h = \frac{K^2 + (1 - 2K)r + (K-1)\gamma}{K^2} \tag{35}$$

We use Corollary 1 to provide comparisons with the centralized case (Section III-D) and to discuss the effect of task similarity (Section III-E and Section III-F).

D. Comparisons with the centralized continual learning

Here we compare the results in Corollary 1 with the expressions for the centralized continual learning setting of [18] in the overparametrized case, i.e. $p > n + 1$. With only one node, i.e., $K = 1$ and $p_k = p$, the same noise level over all tasks, i.e., $\sigma_t^2 = \sigma^2$, focusing on the solution obtained after seeing the last task, i.e., $t = T$, and $T_c = 1$, then our scenario reduces to the setting of [18]. In this setting, CoCoA finds the convergence point of the stochastic gradient descent (SGD), i.e., the smallest-norm of the change of parameters as in [18, Eqn.4]. In particular, for this setting, CoCoA finds the solution of the optimization problem $\min_{\hat{w}_t} \|\hat{w}_t - \hat{w}_{t-1}\|^2$ s.t. $A_t \hat{w}_t = y_t$, where $\hat{w}_{t-1}$ is the solution found for task $t-1$. Note that due to overparameterization, there are multiple solutions that satisfy $A_t \hat{w}_t = y_t$. Hence, CoCoA finds the solution that creates the minimum change in the parameter estimate while satisfying $A_t \hat{w}_t = y_t$ for the new task t. As expected, the generalization error in Corollary 1 for $K = 1$ matches that of [18, Theorem 4.1], i.e.,

$$\frac{(1-r)^T}{T} \sum_{i=1}^{T} \|w_i^*\|^2 + \frac{1}{T} \sum_{\tau=1}^{T} r(1-r)^{T-\tau} \sum_{i=1}^{T} \|w_\tau^* - w_i^*\|^2$$
$$+ \frac{p\sigma^2}{p-n-1}(1 - (1-r)^T), \quad (36)$$

where we have presented $G_T(\hat{w}_T^{(T_c)}) - \sigma^2$ to match the definition of the generalization error in [18]. (Note that r in [18] corresponds to $1 - r$ according to our notation.)

E. Task Similarity – Single Model Parameter

The generalization performance depends heavily on the similarity between tasks. We now investigate the generalization error for the limiting case of task similarity where there is one single model parameter for all tasks, i.e. $w_t^* = w^* \; \forall t$.

Theorem 2. *Consider the setting of Theorem 1. If $w_t^* = w^*$ and $\sigma_t^2 = \sigma^2 \; \forall t$, then*

$$G_T\left(\hat{w}_T^{(T_c)}\right) = \|w^*\|_{H_1^{\{T\}}}^2 + \sigma^2 \frac{K^2 + \sum_{\tau=1}^{T} \sum_{k=1}^{K} \gamma_{\tau,k} h_{\tau+1,k}}{K^2}. \quad (37)$$

Furthermore, if $\|w^*\|^2 < \infty$ and for $t = 1, \ldots, T$,

$$n_t < p_{\min} - \frac{K-1}{2K-1} p_{\max} - 1, \quad (38)$$

or

$$n_t > p_{\max} + \frac{K-1}{2K-1} p_{\min} + 1, \quad (39)$$

where $p_{\min} = \min_{k=1,\ldots,K} p_k$, $p_{\max} = \max_{k=1,\ldots,K} p_k$, then

$$\lim_{T \to \infty} \|w^*\|_{H_1^{\{T\}}}^2 = 0. \quad (40)$$

Proof: See Appendix D.

Corollary 2. *Consider the setting of Theorem 2 with $\sigma^2 = 0$. Then, if (38) or (39) is satisfied, the generalization error is zero in the limit of infinitely many tasks.*

Proof: The result follows from Theorem 2 with $\sigma^2 = 0$.

Remark 4. *Let $\sigma^2 = 0$. If $n_t \geq 1$ and $T \to \infty$, then the algorithm effectively processes an infinite number of samples, i.e., $n_t \times T \to \infty$. Since the tasks have the same unknown parameter vector $w^* \in \mathbb{R}^{p \times 1}$ with $p < \infty$, one may expect that the generalization error should be zero unless the condition $p_k \notin [n_t - 1, n_t + 1]$ is violated, see Remark 3. Nevertheless, Eqn. (38)-(39) suggest stricter conditions on the problem dimensions may be needed. Example 1 illustrates this.*

Example 1. We now illustrate Remark 4. In particular, we illustrate that Eqn. (38)-(39) provides non-trivial conditions for zero generalization error. Consider the equal dimensions scenario in Corollary 1 with $\sigma_t^2 = 0$, and $w_t^* = w^*$, $\forall t$. Let $n_t = 15$, $p = 40$ and $K = 2$. Then $\gamma = 15/4 = 3.75$, hence $p_k \notin [n_t - 1, n_t + 1]$ is satisfied but not (38) or (39). Since h of (35) is $h = 1.375$, evaluating (34) for $t = T$ shows that h^T and hence the generalization error $G_T(\hat{w}_T^{(T_c)})$ diverges for $T \to \infty$.

The next example illustrates that by only changing the network structure, one may have zero error instead of $G_T \to \infty$:

Example 2. Consider Example 1 with $K = 10$. Then $h = 0.846$ in (35), hence $h^T \to 0$ and $G_T(\hat{w}_T^{(T_c)}) \to 0$ as $T \to \infty$.

We also consider the limiting case of the training error:

Lemma 3. *Consider the setting of Theorem 2 and $\sigma^2 = 0$. If (38) or (39) holds $\forall t$, and with the independence of A_t with the error $\hat{w}_T^{(T_c)} - w^*$ in the steady-state [59, Ch. 16], then*

$$\lim_{T \to \infty} F_T(\hat{w}_T^{(T_c)}) \approx 0. \quad (41)$$

Proof: See Appendix E.

To summarize, Corollary 2 and Lemma 3 together show that if the local systems at the nodes are sufficiently away from a square system (with conditions stricter than the ones in Remark 3), and the tasks are similar, then both the generalization error and the training error can be made zero over all tasks.

F. Task Similarity – Decomposition of Error

We now investigate task similarity further by taking a closer look at different terms in the error expression. We start with the following intermediate result:

Corollary 3. *Consider the setting of Corollary 1. Assume that*

$$\sigma_i^2 = \sigma^2, \quad (42)$$
$$\|w_i^*\|^2 = E_1, \quad (43)$$
$$\|w_\tau^* - w_i^*\|^2 = E_2 \mathbb{1}_{i \neq \tau}, \quad (44)$$
$$\langle w_\tau^* - w_i^*, -w_i^* \rangle = E_3 \mathbb{1}_{i \neq \tau}, \quad (45)$$
$$\langle w_\tau^* - w_i^*, w_j^* - w_i^* \rangle = E_4 \mathbb{1}_{j \neq i \neq \tau \neq j}, \quad (46)$$

where $i, \tau, j = 1, \ldots, T$, and $\mathbb{1}_{c(\cdot)} = 1$ if $c(\cdot)$ is true, and 0 otherwise. Then, the expected generalization error for $t = T$ in (34) can be rewritten as

$$G_T\left(\hat{w}_T^{(T_c)}\right) = \psi_0 \sigma^2 + \psi_1 E_1 + \psi_2 E_2 + \psi_3 E_3 + \psi_4 E_4, \quad (47)$$

where

$$\psi_0 = 1 + \frac{\gamma}{K}\frac{1-h^T}{1-h}, \tag{48}$$

$$\psi_1 = h^T, \tag{49}$$

$$\psi_2 = \frac{r+(K-1)\gamma}{K^2}\frac{T-1}{T}\frac{1-h^T}{1-h}, \tag{50}$$

$$\psi_3 = 2\frac{(K-1)(r-\gamma)}{K^2}\frac{T-1}{T}\frac{h^T-b^T}{h-b}, \tag{51}$$

$$\psi_4 = 2\frac{(K-1)(r-\gamma)}{K^2}\frac{T-2}{T}\left(\frac{1-h^T}{1-h}-\frac{b^T-h^T}{b-h}\right), \tag{52}$$

for $h \neq 1$ and $b \neq h$, where h is defined in (35) and $b = 1 - \frac{r}{K}$. If $K = 1$ and $r = 1$, then $h = b = 0$, and ψ_0-ψ_2 are given by (48)-(50), and $\psi_3 = \psi_4 = 0$.

Proof: The result follows from Corollary 1 with algebraic manipulations.

In order to systematically study the task similarity, we introduce the following model for the task parameters:

Task Model 1. Let $0 \leq p_S \leq p$. The unknown vectors $\boldsymbol{w}_t^*$ share the first p_S entries,

$$\boldsymbol{w}_t^* = \begin{bmatrix} \bar{\boldsymbol{w}}^* \\ \bar{\boldsymbol{w}}_t^* \end{bmatrix}, \tag{53}$$

where $\bar{\boldsymbol{w}}^* \in \mathbb{R}^{p_S \times 1}$ is the same for all tasks, and $\bar{\boldsymbol{w}}_t^* \in \mathbb{R}^{(p-p_S) \times 1}$ is specific to each task t. Here, $\bar{\boldsymbol{w}}^*$, and $\bar{\boldsymbol{w}}_1^*, \ldots, \bar{\boldsymbol{w}}_T^*$, are zero-mean and statistically independent. Hence, $\mathbb{E}_{\mathcal{W}}[(\bar{\boldsymbol{w}}_i^*)^\mathsf{T}\bar{\boldsymbol{w}}_\tau^*] = 0, i \neq \tau$, where $\mathcal{W}$ denotes the joint probability distribution function of the parameters, i.e., $(\bar{\boldsymbol{w}}^*, \bar{\boldsymbol{w}}_1^*, \ldots, \bar{\boldsymbol{w}}_T^*) \sim \mathcal{W}$. The covariance matrices of $\bar{\boldsymbol{w}}^*$ and $\bar{\boldsymbol{w}}_t^*$ are given by $\sigma_w^2 \boldsymbol{I}_{p_S}$ and $\sigma_w^2 \boldsymbol{I}_{p-p_S}$, respectively. Hence, the variable p_S, which specifies the number of shared unknowns between the tasks and controls the relative power of the shared component $\bar{\boldsymbol{w}}^*$, is providing a measure of the task similarity for a fixed p. We have

$$\mathbb{E}_{\mathcal{W}}\left[\|\boldsymbol{w}_i^*\|^2\right] = E_w \tag{54}$$

$$\mathbb{E}_{\mathcal{W}}\left[\|\boldsymbol{w}_\tau^* - \boldsymbol{w}_i^*\|^2\right] = 2\frac{p-p_S}{p}E_w, i \neq \tau, \tag{55}$$

$$\mathbb{E}_{\mathcal{W}}\left[\langle \boldsymbol{w}_\tau^* - \boldsymbol{w}_i^*, -\boldsymbol{w}_i^*\rangle\right] = \frac{p-p_S}{p}E_w, i \neq \tau, \tag{56}$$

$$\mathbb{E}_{\mathcal{W}}\left[\langle \boldsymbol{w}_\tau^* - \boldsymbol{w}_i^*, \boldsymbol{w}_j^* - \boldsymbol{w}_i^*\rangle\right] = \frac{p-p_S}{p}E_w, j \neq i \neq \tau \neq j, \tag{57}$$

where $E_w = p\sigma_w^2$.

Corollary 4. *Under the setting of Corollary 1, the expected value of the generalization error under Task Model 1, i.e., $\mathbb{E}_{\mathcal{W}}[G_T(\hat{\boldsymbol{w}}_T^{(T_c)})]$, is given by*

$$\psi_0\sigma^2 + \left(\psi_1 + \frac{p-p_S}{p}\left(2\psi_2 + \psi_3 + \psi_4\right)\right)E_w. \tag{58}$$

Proof: The result follows by taking the expectation of both sides of (34) with respect to $\mathcal{W}$, which results in an expression in the form of (47) where $E_1 - E_4$ in (43) – (46) are substituted with the values in (54) – (57).

We now illustrate the performance under Task Model 1 for different K and T values. For a CoCoA solution $\hat{\boldsymbol{w}}$ obtained
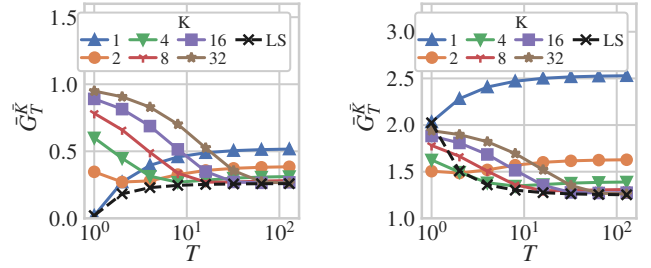
(a) $\sigma^2 = 0.01$ (high SNR) (b) $\sigma^2 = 1$ (low SNR)

Fig. 2: The expected error $\bar{G}_T^{\bar{K}}$ versus T under Task Model 1, with $p = 32$, $p_S = 24$, $n_t = 64$, $T_c = 1$, and $E_w = 1$.

with $K = \bar{K}$ nodes, we denote the error as

$$\bar{G}_T^{\bar{K}} = \mathbb{E}_{\mathcal{W}}\left[G_T\left(\hat{\boldsymbol{w}}_T^{(T_c)}\right)\right], \tag{59}$$

with the convention $\bar{G}_\infty^{\bar{K}} = \lim_{T\to\infty} \mathbb{E}_{\mathcal{W}}\left[G_T\left(\hat{\boldsymbol{w}}_T^{(T_c)}\right)\right]$. We have

$$\bar{G}_\infty^{\bar{K}} = \left(1 + \frac{\gamma}{K}\frac{1}{1-h}\right)\sigma^2 + \frac{2r}{K}\frac{1}{1-h}\left(\frac{p-p_S}{p}E_w\right), \tag{60}$$

under $|h| < 1$. The condition $|h| < 1$ is satisfied for a wide range of p, n_t, K combinations, e.g., under the conditions in (38) and (39). One such scenario is presented in Example 3. Considering $\bar{G}_\infty^{\bar{K}} - \sigma^2$, we observe that both the noise level (σ^2) and the average power of the non-shared part of task unknown vectors $(((p-p_S)/p) \times E_w)$ is scaled with a coefficient in the form of $\alpha/(K(1-h))$ where $\alpha = \gamma$ and $\alpha = 2r$ for the noise and signal components, respectively.

The following example illustrates that in the under-parametrized case, CoCoA can provide lower error than the online centralized continual learning solution for large T.

Example 3. Consider the setting of Corollary 4 with $n_t = 2p$, $p \geq 2$, $T_c = 1$. Under Task Model 1, we have

$$\bar{G}_\infty^1 = \left(1 + \frac{p}{p-1}\right)\sigma^2 + \left(2\frac{p-p_S}{p}E_w\right), \tag{61}$$

$$\bar{G}_\infty^p = \left(1 + \frac{p}{4p-3}\frac{1}{p-1}\right)\sigma^2 + \frac{2p}{4p-3}\left(2\frac{p-p_S}{p}E_w\right), \tag{62}$$

which have been obtained by inserting the values of r, γ and h determined by n_t, p and K used here. The expressions $\bar{G}_\infty^1$ in (61) and $\bar{G}_\infty^p$ in (62) give the expected generalization error under Task Model 1 for the centralized continual learning setting $K = 1$ and the distributed setting with $K = p$, respectively. Comparing the error in (62), i.e., for $K = p$, and the error in (61), i.e., for $K = 1$, we observe that the error is lower in the distributed setting of $K = p$ than in the centralized setting of $K = 1$, regardless of the value of p_S. We also note that when there is no noise, i.e., $\sigma^2 = 0$, the error under $K = p$ converges to $\approx \frac{p-p_S}{p}E_w$ when $T \to \infty$, which is the average power of the non-shared part of the task parameters. Hence, CoCoA finds the shared part of the task unknowns despite its iterative and distributed nature.

In Fig. 2 and Fig. 3, we present $\bar{G}_T^{\bar{K}}$ versus T under Task Model 1 for $p = 32$, $p_S = 24$, for the underparametrized and overparametrized scenarios, respectively. The curve with the
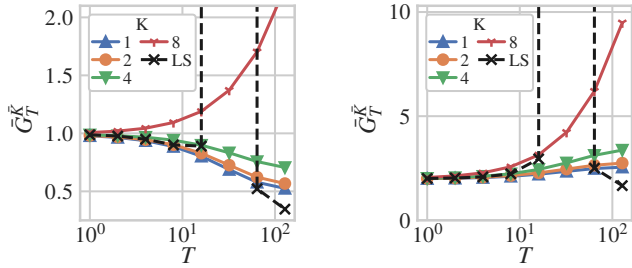
(a) $\sigma^2 = 0.01$ (high SNR)   (b) $\sigma^2 = 1$ (low SNR)

Fig. 3: The expected error $\bar{G}_T^{\bar{K}}$ versus T under Task Model 1, with $p = 32$, $p_S = 24$, $n_t = 1$, and $E_w = 1$.

legend "LS" plots the error of the least-squares (LS) benchmark presented in Section II-E and is obtained numerically, whereas the other curves are plotted using Corollary 4. We note that the high error values for the LS solution around $T = 32$ in Fig. 3 is due to the ill-conditioning of the system for $Tn_t \approx p$, similar to the scenarios in Remark 3. Fig. 2 illustrates that the CoCoA solutions can achieve error values that are close to that of the LS solution for large T and large K; and can even obtain error values lower than the LS solution for small T under low SNR (Fig. 2b). In Fig. 3, we observe that the error values of CoCoA are close to those of the LS solution for small and moderate T ($1 \lesssim T \lesssim 10$) for most K. Fig. 3 illustrates that the error of CoCoA for large T ($T \gtrsim 16$) can decrease or increase with increasing T depending on the noise level and K, although the lowest error values for the LS solution across different T are obtained with the large value of $T \approx 100$.

IV. NUMERICAL RESULTS

We now present numerical results in order to to illustrate the continual learning performance of CoCoA and the analytical results of Section III.

We include an experiment with real-world data in Section IV-F whose details are explained therein. In the rest of the experiments, we use the following setting: For each experiment, we generate a set of task unknowns $\boldsymbol{w}_t^*$, $\forall t$. In order to control the task similarity, we use the variable p_S, as in (53), where the unknown vectors $\boldsymbol{w}_t^*$ share the first p_S entries, where $\bar{\boldsymbol{w}}^* \in \mathbb{R}^{p_S \times 1}$ is the same for all $\boldsymbol{w}_t^*$, and $\bar{\boldsymbol{w}}_t^* \in \mathbb{R}^{(p-p_S) \times 1}$ is independently generated for each t. We draw $\bar{\boldsymbol{w}}^*$ and $\bar{\boldsymbol{w}}_t^*$ from the standard Gaussian distribution, and normalize the drawn vectors such that $\|\bar{\boldsymbol{w}}^*\|^2 = \frac{p_S}{p}$ and $\|\bar{\boldsymbol{w}}_t^*\|^2 = \frac{p-p_S}{p}$. Hence, $\|\boldsymbol{w}_t^*\|^2 = 1$.

The entries of the regressors matrices $\boldsymbol{A}_t$ are generated i.i.d. from $\mathcal{N}(0,1)$, hence Assumption 1 is fulfilled. The noise vectors $\boldsymbol{z}_t$ are independently drawn from $\mathcal{N}(0, \sigma_t^2 \boldsymbol{I}_{n_t})$, where σ_t^2 may vary over different experiments. The observations $\boldsymbol{y}_t$ are generated as in (1), i.e., $\boldsymbol{y}_t = \boldsymbol{A}_t \boldsymbol{w}_t^* + \boldsymbol{z}_t$. We have $p_k = \frac{p}{K}$, $\forall k$. With $\hat{\boldsymbol{w}}_0^{(0)} = \boldsymbol{0}$, we run Algorithm 1 for $t = 1, \dots, T$ to obtain the estimate $\hat{\boldsymbol{w}}_T^{(T_c)}$, trained over all tasks. We then compute the generalization error as $g_T(\hat{\boldsymbol{w}}_T^{(T_c)})$ in (10), and create an average over 100 i.i.d. sets of training data to report the empirical value of $G_T(\hat{\boldsymbol{w}}_t^{(T_c)})$.
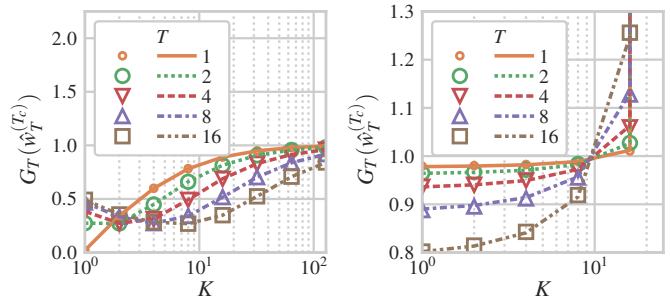
(a) $n_t = 2048$, $\sigma_t^2 = 0.01$, $T_c = 1$. (b) $n_t = 32$, $\sigma_t^2 = 0.01$, $T_c = 100$.

Fig. 4: The generalization error versus the number of nodes, for different number of tasks (marker: analytical, line: simulations). Here, $p = 1024$, $p_S = 768$.

A. Verification of Theorem 1 and Effect of Network Size

In Fig. 4 we plot the generalization error $G_T(\hat{\boldsymbol{w}}_T^{(T_c)})$ versus the number of nodes in the network K, for different numbers of tasks T. The x-axis shows the number of nodes K and is sampled at $\{2^0, 2^1, 2^2, \dots\}$. For both figures, $p = 1024$, $p_S = 768$ and $\sigma_t^2 = 0.01$. In Fig. 4a, $n_t = 2048$ and $T_c = 1$, thus Assumption 3 is fulfilled, i.e., $T_c = 1$. In Fig. 4b, $n_t = 32$ and $T_c = 100$, thus Assumption 2 is fulfilled for $K < 32$, i.e., $p_k > n_t + 1$, $\forall t, k$.

We plot the average generalization error obtained via simulations (lines), together with the analytically evaluated expected generalization error by Theorem 1 (markers). We observe that analytical and empirical results match both in Fig. 4a and 4b, i.e., either under Assumption 2 or Assumption 3.

We observe that the number of nodes K has a non-trivial effect on the generalization error. For instance, in Fig. 4a, the error first decreases (for $T \geq 2$) as the number of nodes K increases, and then increases to approach $\frac{1}{T}\sum_{t=1}^T \|\boldsymbol{w}_t\|^2 + \sigma_t^2 = 2$, which is the generalization error of the zero-estimator $\hat{\boldsymbol{w}} = \boldsymbol{0}$. The behaviour with K is closely related to the task similarity, which is discussed in Section IV-B. The generalization error in Fig. 4b increases gradually with K up to $K = 16$, where the error starts to increase rapidly due to local ill-conditioning for $p_k \approx n_t$, see Remark 3.

We now compare generalization performance of CoCoA with the performance of the offline and centralized solution $\hat{\boldsymbol{w}}_{\text{LS}}$ in (19). The error associated with $\hat{\boldsymbol{w}}_{\text{LS}}$ in (19) for $T = 1, 2, 4, 8, 16$, is given by $\approx \{0.02, 0.18, 0.22, 0.25, 0.25\}$ for Fig. 4a and $\approx \{0.98, 0.97, 0.94, 0.90, 0.87\}$ for Fig. 4b. We observe that in some but not all scenarios, by tuning the number of nodes K for a given number of tasks T, one may obtain close or even lower values of expected generalization error with CoCoA in comparison to the offline and centralized solution $\hat{\boldsymbol{w}}_{\text{LS}}$. For instance, in Fig. 4b for $T = 16$ and $K = 2$ the CoCoA error is 0.81, which is lower than 0.87 for $\hat{\boldsymbol{w}}_{\text{LS}}$.

We observe that the error behaviour with the number of tasks T depends on the number of nodes K, and is affected by the tasks' similarities, which is investigated in Section IV-B.
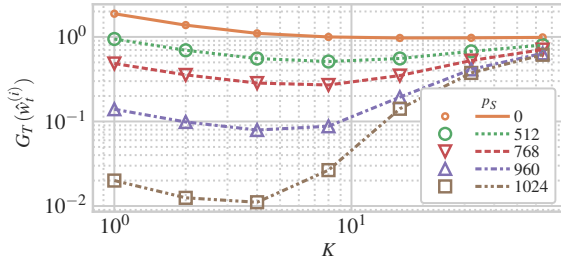
Fig. 5: The generalization error versus the number of nodes, for different number of shared task unknowns p_S, i.e., task similarity (marker: analytical, line: simulations). Here, $n_t = 2048$, $p = 1024$, $\sigma_t^2 = 0.01$, $T = 16$, $T_c = 1$.

(a) $K = 4$ (b) $K = 16$
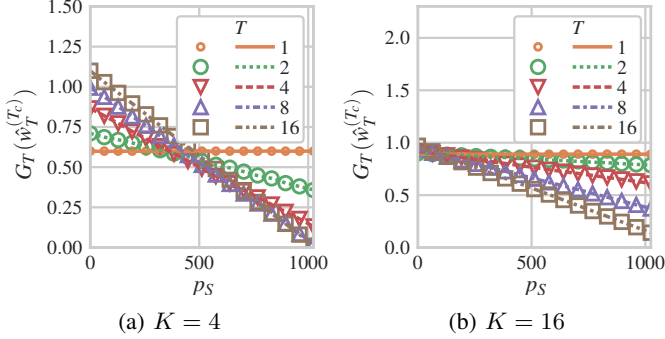
Fig. 6: The generalization error versus the number of shared task unknowns p_S, i.e., task similarity (marker: analytical, line: simulations). Here, $n_t = 2048$, $p = 1024$, $\sigma_t^2 = 0.01$, $T_c = 1$.

B. Generalization Error and Task Similarity

In Fig. 5, we plot the generalization error versus the number of nodes K for different levels of similarity, i.e., number of shared parameters p_S. Here, $n_t = 2048$, $p = 1024$, $\sigma_t^2 = 0.01$, $T = 16$, and $T_c = 1$, thus Assumption 3 is fulfilled. We again observe a match between the analytical and simulated error curves as we vary p_S and K. This figure quantifies the possible large impact of task similarity on the generalization performance; and the dependence of this impact on the network size K. Compared to having no shared parameters between the tasks ($p_S = 0$), more similarity (larger p_S) decreases the generalization error. In particular, for $p_S = 1024$, i.e. the parameter vector is the same for all tasks, the error for $K = 4$ is close to the noise floor of $\sigma_t^2 = 0.01$. For large K, the increase in the error with increasing K is consistent with the fact that with too many nodes, the number of possibly incompatible local estimates becomes too high, hence more rounds of communications may be needed to reach compatibility between these large number of local estimates.

We plot the generalization error versus the number of shared parameters p_S with varying numbers of tasks T for $K = 4$ and $K = 16$ in Fig. 6a and Fig. 6b, respectively. These plots quantify how for dissimilar tasks, i.e., small p_S, the error increases with the number of tasks T, and for similar tasks, i.e., large p_S, the error decreases as the number of tasks increases. This is consistent with the fact that it may be possible to obtain good estimates with a model with a single parameter vector if the tasks are sufficiently similar; and that with a
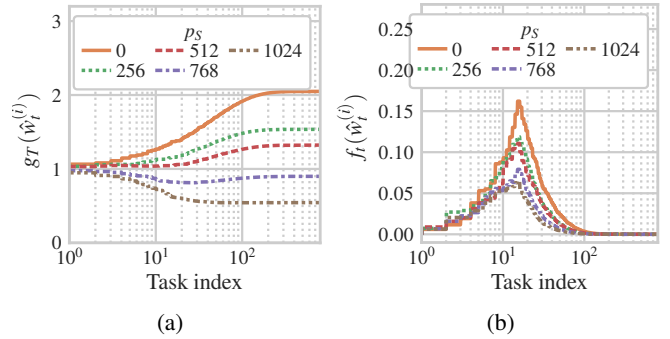
(a)   (b)

Fig. 7: The generalization error (a) and training error (b) for the estimate $\hat{\boldsymbol{w}}_t^{(i)}$ versus the task index, i.e., seen tasks, for different numbers of shared unknowns p_S. Here, $n_t = 32$, $p = 1024$, $\sigma_t^2 = 0.01$, $K = 2$, $T_c = 100$, $T = 16$.

(a)   (b)
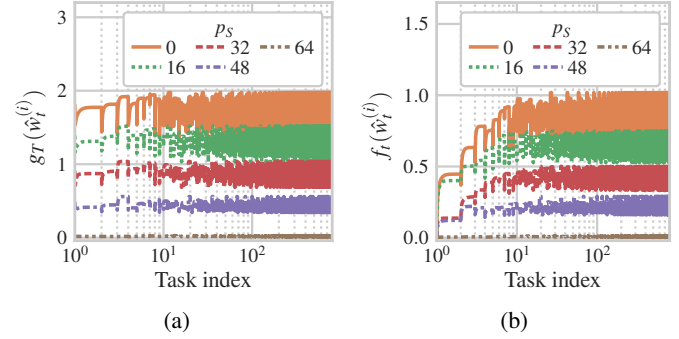
Fig. 8: The generalization error (a) and training error (b) for the estimate $\hat{\boldsymbol{w}}_t^{(i)}$ versus the task index, i.e., seen tasks, for different numbers of shared unknowns p_S. Here, $n_t = 128$, $p = 64$, $\sigma_t^2 = 0.01$, $K = 2$, $T_c = 100$, $T = 16$.

larger T, the effective number of observations seen by CoCoA increases, which then can be used to estimate this single parameter vector. Comparing Fig. 6a and Fig. 6b, we observe that the network size K affects the range of p_S on which the curves cross, i.e., for which p_S a larger number of tasks T is beneficial. For a large number of nodes K (Fig. 6b), continual learning with $T > 1$ with tasks that are even dissimilar, i.e. small p_s, can provide relatively good performance compared to the case with $T = 1$.

C. Learning Curves

In Fig. 7 and 8, we study the evolution of the generalization error and the training error as the the model is repeatedly trained on the tasks $t = 1, \ldots, T$. In particular, we plot $g_T(\hat{\boldsymbol{w}}_t^{(i)})$ and $f_t(\hat{\boldsymbol{w}}_t^{(i)})$, see (10) and (4), respectively. The estimate $\hat{\boldsymbol{w}}_T^{(T_c)}$ does not necessarily converge after training on all tasks once, hence we repeat the tasks after all T tasks have been trained upon. The resulting task sequence is $t' = 1, \ldots, T, 1, \ldots, T, \ldots$, where t' corresponds to the task index on the x-axes in Fig. 7 and 8. For each task index t', we plot the error over the T_c iterations of CoCoA, hence there are T_c points in between every integer task index.

In Fig. 7, $T_c = 100$, $\sigma_t^2 = 0.01$, $T = 16$, $n_t = 32$, $p = 1024$, $K = 2$. Hence, $p_k = 512 > n_t = 32$, and Assumption 2 is fulfilled and Lemma 2 holds, i.e., CoCoA

converges in the first iteration. Accordingly, in Fig. 7, the generalization and training error are constant over the CoCoA iterations between each integer task index. Furthermore, these plots provide insights into the interplay between the level of task similarity and the number of tasks. We observe that if the similarity is relatively low, e.g., for $p_S = 0, 256, 512$, then the generalization error in Fig. 7a increases for each task trained upon. On the other hand, the training error in Fig. 7b decreases as the task index increases after $T = 16$, i.e., after all tasks have been trained on once. This effect is consistent with overfitting to training data under the locally overparameterized setting of $p_k = 512 > n_t = 32$, i.e., the model becomes good at predicting the seen samples of data, while generalizing poorly.

In Fig. 8, we repeat the experiment of Fig. 7, but $n_t = 128$ and $p = 64$. As $K = 2$, we have $p_k < 128$, hence Lemma 2 does not hold, and we observe a learning transient for each seen task, i.e., the error curves between each integer task index. After training on all $T = 16$ tasks, both the generalization and training errors fluctuate around fixed mean values, and the mean generalization error for a given p_S improves as p_S increases.

D. Effect of the Number of Iterations T_c

In Fig. 9, we plot the generalization error versus the number of samples per task n_t for different number of tasks T, for both $T_c = 1$ and $T_c = 100$ iterations per task. Here, $\sigma_t^2 = 0.01$, $K = 32$, $p = 1024$, $p_S = 512$.

Since $p_k = \frac{p}{K} = 32$, for $n_t < 32$ the curves for $T_c = 1$ and $T_c = 100$ are on top of each other due to the convergence of CoCoA in the first iteration $i = 1$, see Remark 1. As n_t increases toward $n_t = 32$, there is a large peak in the error for $p_k \approx n_t$, since the local problems are now at the interpolation threshold, hence ill-conditioned, see Remark 3.

For $n_t \geq 32$, the error decreases again with increasing n_t, and the curves for $T_c = 1$ and $T_c = 100$ exhibit different behaviour. Here, the behaviour is different between the pairs of curves for different number of tasks T. In particular, if $T = 1$, then the error is lower with high T_c, and if there are many tasks, i.e., if $T = 16$, the relation is flipped and the error is higher with higher T_c. Hence, if there are many tasks with not enough task similarity, it may be beneficial in terms of generalization error to run CoCoA for a smaller number of iterations, i.e., apply early stopping, for each task.

E. Effect of Feature Correlation

We now investigate the effect of feature correlation. The covariance matrices of the regressors are symmetric Toeplitz matrices where the first row is given by $[\varepsilon^0, \varepsilon^1, \dots \varepsilon^{(p-1)}]$ where $0 \leq \varepsilon \leq 1$. Hence, increasing values of ε results in higher values of correlation between features. We consider the setting in Fig. 4 with $T = 8$. The resulting plots are provided in Fig. 10. In general, lower error values are obtained for higher values of correlation although exceptions to this trend exist, e.g., Fig. 10a for $\varepsilon = 0.5, 0.95$ and small K. Similar to Fig. 4b, the error in Fig. 10b rapidly increases with $K = 16$ where we
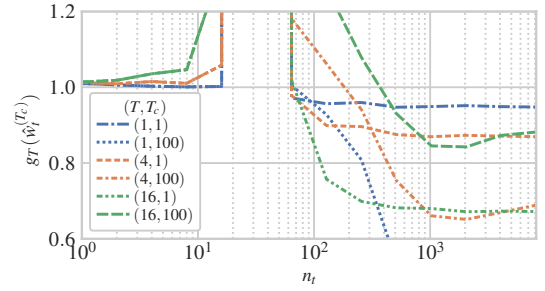
Fig. 9: The generalization error versus number of samples per task n_t, for different number of tasks T and number of iterations T_c of CoCoA. Here, $K = 32$, $p = 1024$, $p_S = 512$, $\sigma_t^2 = 0.01$.
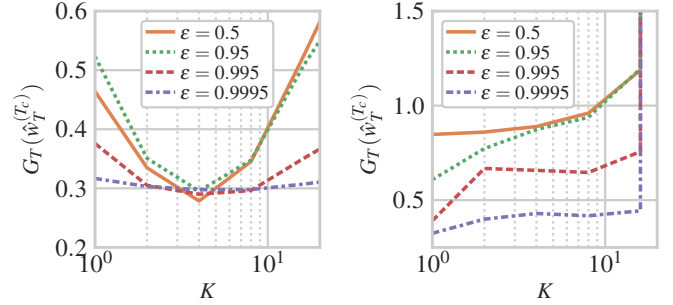
(a) $n_t = 2048$, $\sigma_t^2 = 0.01$, $T_c = 1$. (b) $n_t = 32$, $\sigma_t^2 = 0.01$, $T_c = 100$.

Fig. 10: The generalization error versus the number of nodes K, for different levels of correlation. Here, $p = 1024$, $p_S = 768$, $T = 8$.

get closer to the case of $p_k \approx n_t$; highlighting the importance of Remark 3 also under correlated regressors.

F. Continual Learning on MNIST with CoCoA

We now study the continual learning performance of CoCoA using the MNIST dataset [60]. This dataset consists of images of the handwritten digits with labels from "0" to "9". We consider the following domain incremental learning setting [41, Figure 1, Table 2], [61]: We split the data into tasks by separating the samples into the following $T = 5$ tasks ("0", "1"), ("2", "3"), ("4", "5"), ("6", "7"), ("8", "9"), i.e., each of the $T = 5$ tasks consists of samples of one even digit and one
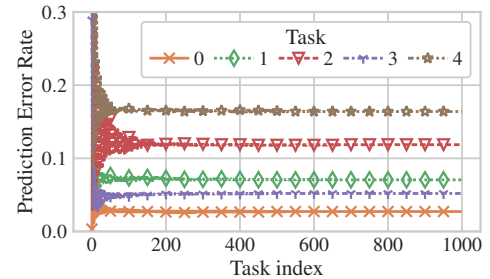
Fig. 11: The test prediction error rate for the odd/even MNIST classification task when trained with quadratic loss, versus the number of repetitions of Algorithm 1. Here, $K = 2$, $p = 3 \cdot 10^3$, $n_t = 100$, and $T_c = 1$.
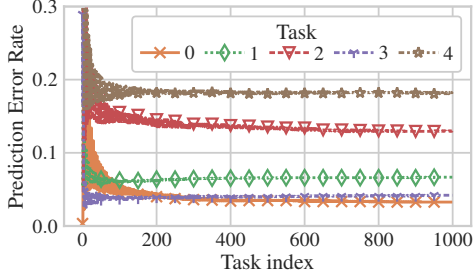
Fig. 12: The test prediction error rate for the odd/even MNIST classification task when trained with logistic loss, versus the number of repetitions of Algorithm 1. Here, $K = 2$, $p = 3 \cdot 10^3$, $n_t = 100$, and $T_c = 1$.

odd digit. Hence, the continual learning task is to determine whether a given digit is even or odd when trained on sets of distinct pairs of even and odd digits.

We convert the 28×28 pixel images, with pixel values on $[0, 255]$, to 784×1 vectors $\boldsymbol{x}_j \in \mathbb{R}^{784 \times 1}$, with the values divided by 255 such that entries of $\boldsymbol{x}_j$ lie on $[0, 1]$. Using random features [62] the vectors $\boldsymbol{x}_j$ are transformed to regressors as $\boldsymbol{a}_j = [\cos(\boldsymbol{\zeta}_1^T \boldsymbol{x}_j), \cdots, \cos(\boldsymbol{\zeta}_p^T \boldsymbol{x}_j)]^\mathsf{T} \in \mathbb{R}^{p \times 1}$, where $\boldsymbol{\zeta}_\ell \in \mathbb{R}^{784 \times 1}$ are i.i.d. random vectors with $\boldsymbol{\zeta}_\ell \sim \mathcal{N}(\boldsymbol{0}, 0.04\boldsymbol{I}_{784})$. We use CoCoA to train a model $\hat{\boldsymbol{w}}_{\text{odd},t}^{(T_c)} \in \mathbb{R}^{p \times 1}$ on the odd digits, and one model $\hat{\boldsymbol{w}}_{\text{even},t}^{(T_c)} \in \mathbb{R}^{p \times 1}$ on the even digits in a continual learning setting. We apply the one-v.s.-rest classification strategy [63] to create predictions of the labels. We report the prediction error rate for each task using test sets of 2000 samples unseen during training. We use two different cost functions for training, the quadratic loss of (2), and the logistic loss $\ell(\hat{\boldsymbol{w}}) = \sum_{j=1}^{n} \ln\left(1 + e^{-y_j \boldsymbol{a}_j^\mathsf{T} \hat{\boldsymbol{w}}}\right)$, where $y_j \in \{-1, 1\}$ is the label that corresponds to $\boldsymbol{a}_j$.

With $p = 3000$, $n_t = 100$, $K = 2$, $T_c = 1$, the $T = 5$ tasks, and 100 training repetitions over the task sequence $t = 1, \ldots, T$, we plot the prediction error rate per task versus the training iteration index in Fig. 11 for the quadratic loss and Fig. 12 for the logistic loss. Here, task 0 corresponds to ("0","1"), task 1 to ("2", "3"), etc. Although some of the tasks (e.g. Task 0: "0" v.s."1") are giving significantly lower error rate than others (e.g. Task 4: "8" v.s."9"), CoCoA is able to perform significantly better than the random chance of 0.5 for all tasks when trained with the quadratic loss or the logistic loss.

V. DISCUSSIONS

Our results show that generalization performance heavily depends on the number of nodes K. Hence, one would want to optimize the performance of CoCoA by adjusting K, but this may not be possible in all applications. In these cases, avoiding the undesirable conditions mentioned in Remark 3 and (38) – (39) by assigning different number of parameters to each node, using a subset of available nodes or adjusting the model size can be beneficial. Regularization can also be utilized to prevent the high-error values at the interpolation threshold at the cost of slow convergence rate [40, Fig. 8].

Our analytical characterizations focus either on the over-parametrized local models (Assumption 2) or the one-shot setting (Assumption 3). On the other hand, an important trade-off within distributed learning is the one between the number of communication rounds and the amount of local computations. The CoCoA framework is flexible in terms of this trade-off as it allows local solvers to be run to an arbitrary level of accuracy. Extending our analysis to explore the consequences of this flexibility for continual learning is a promising research direction.

VI. CONCLUSIONS

We have focused on continual learning with the distributed optimization algorithm CoCoA and provided analytical expressions for the generalization error for a range of scenarios. These results revealed that under continual learning, the network structure may significantly affect the generalization error in a manner that goes beyond what has been reported with only one task in distributed learning [40] and centralized continual learning [18]. We have quantified how the most favorable network structure for good generalization performance, such as the number of nodes in the network, depends on the task similarity as well as the number of tasks.

Characterizing the continual learning performance under general regressor models including correlation between features, different communications schemes for CoCoA and also for other distributed learning algorithms are considered important directions for future work.

APPENDIX

A. Preliminaries

The following lemma collects some properties of Gaussian random matrices that are used throughout the derivations:

Lemma 4. *If* $\boldsymbol{A}_t = [\boldsymbol{A}_{t,[1]}, \cdots, \boldsymbol{A}_{t,[K]}]$, *and* $\boldsymbol{A}_{t,[k]} \in \mathbb{R}^{n_t \times p_k}$, *with* $p_k \notin [n_t - 1, n_t + 1]$, *and* $p_k, n_t \geq 1$ $k = 1, \ldots, K$, *are all standard Gaussian random matrices, then*

$$\mathbb{E}_{\boldsymbol{A}_{t,[k]}}\left[\boldsymbol{A}_{t,[k]}^\mathsf{T} \boldsymbol{A}_{t,[k]}\right] = n_t \boldsymbol{I}_{p_k}, \tag{63}$$

$$\mathbb{E}_{\boldsymbol{A}_{t,[k]}}\left[\boldsymbol{A}_{t,[k]}^{+} \boldsymbol{A}_{t,[k]}\right] = r_{t,k} \boldsymbol{I}_{p_k}, \tag{64}$$

$$\mathbb{E}_{\boldsymbol{A}_{t,[k]}}\left[\left(\boldsymbol{A}_{t,[k]} \boldsymbol{A}_{t,[k]}^\mathsf{T}\right)^{+}\right] = \frac{\gamma_{t,k}}{n_t} \boldsymbol{I}_{n_t}, \tag{65}$$

$$\mathbb{E}_{\boldsymbol{A}_{t,[i]} \boldsymbol{A}_{t,[k]}}\left[\boldsymbol{A}_{t,[i]}^\mathsf{T} \left(\boldsymbol{A}_{t,[k]} \boldsymbol{A}_{t,[k]}^\mathsf{T}\right)^{+} \boldsymbol{A}_{t,[i]}\right] = \gamma_{t,k} \boldsymbol{I}_{p_i}, \tag{66}$$

with $r_{t,k} = \frac{\min(n_t, p_k)}{p_k}$, $\gamma_{t,k} = \frac{\min(n_t, p_k)}{\max(n_t, p_k) - \min(n_t, p_k) - 1}$, *and* $i \neq k$. *Additionally, if* $\boldsymbol{H} = diag\{h_k \boldsymbol{I}_{p_k}\}_{k=1}^{K} \in \mathbb{R}^{p \times p}$ *is a diagonal matrix with arbitrary* $h_k \in \mathbb{R}$, $k = 1, \ldots, K$, *then the following also hold,*

$$\mathbb{E}_{\boldsymbol{A}_t}\left[\boldsymbol{H} \bar{\boldsymbol{A}}_t \boldsymbol{A}_t\right] = diag\left\{\frac{h_k r_{t,k}}{K} \boldsymbol{I}_{p_k}\right\}_{k=1}^{K}, \tag{67}$$

$$\mathbb{E}_{\boldsymbol{A}_t}\left[\boldsymbol{H} \boldsymbol{P}_t\right] = diag\left\{h_k \left(1 - \frac{r_{t,k}}{K}\right) \boldsymbol{I}_{p_k}\right\}_{k=1}^{K}, \tag{68}$$

$$\mathbb{E}_{\boldsymbol{A}_t}\left[\bar{\boldsymbol{A}}_t^\mathsf{T} \boldsymbol{H} \bar{\boldsymbol{A}}_t\right] = \frac{1}{K^2} \sum_{k=1}^{K} \frac{h_k \gamma_{t,k}}{n_t} \boldsymbol{I}_{n_t}, \tag{69}$$

$$\underset{\boldsymbol{A}_t}{\mathbb{E}}\left[\boldsymbol{A}_t^\intercal\bar{\boldsymbol{A}}_t^\intercal\boldsymbol{H}\bar{\boldsymbol{A}}_t\boldsymbol{A}_t\right]=diag\left\{\frac{h_k r_{t,k}+\sum_{\substack{i=1\\i\neq k}}^{K}h_i\gamma_{t,i}}{K^2}\boldsymbol{I}_{p_k}\right\}_{k=1}^{K}, \quad (70)$$

$$\underset{\boldsymbol{A}_t}{\mathbb{E}}\left[\boldsymbol{P}_t^\intercal\boldsymbol{H}\boldsymbol{P}_t\right]$$

$$=diag\left\{\frac{h_k(K^2+r_{t,k}(1-2K))+\sum_{\substack{i=1\\i\neq k}}^{K}h_i\gamma_{t,i}}{K^2}\boldsymbol{I}_{p_k}\right\}_{k=1}^{K}. \quad (71)$$

Proof: The expression in (63) is a direct consequence of the fact that $\boldsymbol{A}_{t,[k]}\in\mathbb{R}^{n_t\times p_k}$ are standard Gaussian. For (64) see [64, Eqn. (58)], and note that for $p_k < n_t$, $\boldsymbol{A}_{t,[k]}$ is full column-rank and $\boldsymbol{A}_{t,[k]}^{+}\boldsymbol{A}_{t,[k]} = \boldsymbol{I}_{p_k}$. For (65), see [65]. Combining (63) and (65), one obtains (66). We obtain (67) – (71) from (63) – (66) with algebraic manipulations together with the definitions of $\boldsymbol{P}_t$ and $\bar{\boldsymbol{A}}_t$ in Lemma 1. □

The following lemma gives an expression for the average distance of the CoCoA solution $\hat{\boldsymbol{w}}_t^{(T_c)}$ to a given vector $\boldsymbol{u}$ for an arbitrary distribution for $\boldsymbol{A}_i$. We use a version of this result specialized to Gaussian case in the proof of Theorem 1.

Lemma 5. *Let* $\boldsymbol{A}_1, \ldots, \boldsymbol{A}_t, \boldsymbol{z}_1, \ldots, \boldsymbol{z}_t$ *be uncorrelated and the noise vectors* $\boldsymbol{z}_\tau$ *be zero-mean. If all partitions* $\boldsymbol{A}_{\tau,[k]}$, $\tau = 1, \ldots, t$, $k = 1, \ldots, K$, *are full row rank or* $T_c = 1$, *then for any fixed* $\boldsymbol{u}\in\mathbb{R}^{p\times 1}$,

$$\underset{\mathcal{D}_t}{\mathbb{E}}\left[\left\|\hat{\boldsymbol{w}}_t^{(T_c)} - \boldsymbol{u}\right\|^2\right] = \|\boldsymbol{u}\|_{\boldsymbol{H}_1^{\{t\}}}^2 + \sum_{\tau=1}^{t}\alpha_\tau, \quad (72)$$

where

$$\alpha_\tau = \|\boldsymbol{w}_\tau^* - \boldsymbol{u}\|^2_{\underset{\boldsymbol{A}_\tau}{\mathbb{E}}\left[\boldsymbol{A}_\tau^\intercal\bar{\boldsymbol{A}}_\tau^\intercal\boldsymbol{H}_{\tau+1}^{\{t\}}\bar{\boldsymbol{A}}_\tau\boldsymbol{A}_\tau\right]}$$

$$+\underset{\boldsymbol{z}_\tau}{\mathbb{E}}\left[\|\boldsymbol{z}_\tau\|^2_{\underset{\boldsymbol{A}_\tau}{\mathbb{E}}\left[\bar{\boldsymbol{A}}_\tau^\intercal\boldsymbol{H}_{\tau+1}^{\{t\}}\bar{\boldsymbol{A}}_\tau\right]}\right]+2\left\langle\boldsymbol{w}_\tau^*-\boldsymbol{u},\right.$$

$$\left.\sum_{j=0}^{\tau-1}\left(\prod_{\ell=j+1}^{\tau-1}\underset{\boldsymbol{A}_\ell}{\mathbb{E}}\left[\boldsymbol{P}_\ell\right]\right)\underset{\boldsymbol{A}_j}{\mathbb{E}}\left[\boldsymbol{s}_j\right]\right\rangle_{\underset{\boldsymbol{A}_\tau}{\mathbb{E}}\left[\boldsymbol{A}_\tau^\intercal\bar{\boldsymbol{A}}_\tau^\intercal\boldsymbol{H}_{\tau+1}^{\{t\}}\boldsymbol{P}_\tau\right]}, \quad (73)$$

where $\bar{\boldsymbol{A}}_\tau$ *and* $\boldsymbol{P}_\tau$ *are defined in Lemma 1,* $\boldsymbol{H}_{t+1}^{\{t\}} = \boldsymbol{I}_p$, *and*

$$\boldsymbol{H}_\tau^{\{t\}} = \mathbb{E}_{\boldsymbol{A}_\tau,\ldots,\boldsymbol{A}_t}[\boldsymbol{P}_\tau^\intercal\cdots\boldsymbol{P}_t^\intercal\boldsymbol{P}_t\cdots\boldsymbol{P}_\tau], \quad \tau = 1, \ldots, t, \quad (74)$$

and where $\boldsymbol{s}_0 = -\boldsymbol{u}$, *and*

$$\boldsymbol{s}_j = \bar{\boldsymbol{A}}_j\boldsymbol{A}_j(\boldsymbol{w}_j^* - \boldsymbol{u}), \quad j = 1, \ldots, t-1. \quad (75)$$

Proof: See Appendix F.

B. Proof of Lemma 1

From Algorithm 1, $\boldsymbol{v}_{t,[k]}^{(0)} = K\boldsymbol{A}_{t,[k]}\hat{\boldsymbol{w}}_{t,[k]}^{(0)}$, and $\bar{\boldsymbol{v}}_t^{(1)} = \frac{1}{K}\sum_{k=1}^{K}\boldsymbol{v}_{t,[k]}^{(0)} = \boldsymbol{A}_t\hat{\boldsymbol{w}}_t^{(0)}$. Then, $\Delta\hat{\boldsymbol{w}}_{t,[k]}^{(1)} = -\frac{1}{K}\boldsymbol{A}_{t,[k]}^{+}\boldsymbol{A}_t\hat{\boldsymbol{w}}_t^{(0)} + \frac{1}{K}\boldsymbol{A}_{t,[k]}^{+}\boldsymbol{y}_t$, $\hat{\boldsymbol{w}}_{t,[k]}^{(1)} = \hat{\boldsymbol{w}}_{t,[k]}^{(0)} - \frac{1}{K}\boldsymbol{A}_{t,[k]}^{+}\boldsymbol{A}_t\hat{\boldsymbol{w}}_t^{(0)} + \frac{1}{K}\boldsymbol{A}_{t,[k]}^{+}\boldsymbol{y}_t$. Stacking $\hat{\boldsymbol{w}}_{t,[k]}^{(1)}$, as in (14) with $i = 1$,

$$\hat{\boldsymbol{w}}_t^{(1)}= \hat{\boldsymbol{w}}_t^{(0)} - \frac{1}{K}\begin{bmatrix}\boldsymbol{A}_{t,[1]}^{+}\\\vdots\\\boldsymbol{A}_{t,[K]}^{+}\end{bmatrix}\boldsymbol{A}_t\hat{\boldsymbol{w}}_t^{(0)} + \frac{1}{K}\begin{bmatrix}\boldsymbol{A}_{t,[1]}^{+}\\\vdots\\\boldsymbol{A}_{t,[K]}^{+}\end{bmatrix}\boldsymbol{y}_t. \quad (76)$$

Inserting the initialization $\hat{\boldsymbol{w}}_t^{(0)} = \hat{\boldsymbol{w}}_{t-1}^{(T_c)}$, we obtain (20).

The expression in (23) is obtained by adding and subtracting $\bar{\boldsymbol{A}}_t\boldsymbol{A}_t\boldsymbol{u}$ to $\hat{\boldsymbol{w}}_t^{(1)} - \boldsymbol{u}$, and opening up $\boldsymbol{y}_t = \boldsymbol{A}_t\boldsymbol{w}_t^* + \boldsymbol{z}_t$ and re-arranging. This concludes the proof.

C. Proof of Theorem 1

The expected generalization error, defined in (12), is

$$G_T(\hat{\boldsymbol{w}}_t^{(T_c)}) = \frac{1}{T}\sum_{i=1}^{T}\underset{\mathcal{D}_t}{\mathbb{E}}\left[\|\hat{\boldsymbol{w}}_t^{(T_c)} - \boldsymbol{w}_i^*\|^2\right] + \sigma_i^2. \quad (77)$$

We will show that, with the definitions given in Theorem 1,

$$\underset{\mathcal{D}_t}{\mathbb{E}}\left[\left\|\hat{\boldsymbol{w}}_t^{(T_c)} - \boldsymbol{w}_i^*\right\|^2\right] = \|\boldsymbol{w}_i^*\|_{\boldsymbol{H}_1^{\{t\}}}^2 + \phi\left(\hat{\boldsymbol{w}}_t^{(T_c)}, \boldsymbol{w}_i^*\right). \quad (78)$$

Lemma 5 gives this expression up to the expectations over the distributions of regressors and noise vector, with

$$\phi\left(\hat{\boldsymbol{w}}_t^{(T_c)}, \boldsymbol{w}_i^*\right) = \sum_{\tau=1}^{t}\alpha_\tau, \quad (79)$$

where we use $\boldsymbol{u} = \boldsymbol{w}_i^*$ in α_τ.

We now continue with deriving the expectations of the expressions in Lemma 5, in the setting of Theorem 1.

The matrices $\boldsymbol{P}_\tau = \boldsymbol{I}_p - \bar{\boldsymbol{A}}_\tau\boldsymbol{A}_\tau$, $1 \leq \tau \leq t$, are uncorrelated and we have $\boldsymbol{H}_1^{\{t\}} = \underset{\mathcal{D}_{t-1}}{\mathbb{E}}\left[\boldsymbol{P}_1^\intercal\cdots\boldsymbol{P}_{t-1}^\intercal\boldsymbol{H}_t^{\{t\}}\boldsymbol{P}_{t-1}\cdots\boldsymbol{P}_1\right]$, with $\boldsymbol{H}_t^{\{t\}} = \underset{\boldsymbol{A}_t}{\mathbb{E}}\left[\boldsymbol{P}_t^\intercal\boldsymbol{P}_t\right] = diag\{h_{t,k}\boldsymbol{I}_{p_k}\}_{k=1}^{K}$, where

$$h_{t,k} = \frac{K^2 + r_{t,k}(1 - 2K) + \sum_{\substack{i=1\\i\neq k}}^{K}\gamma_{t,i}}{K^2}, \quad (80)$$

by (71). We can repeat this for $\boldsymbol{H}_{t-1}^{\{t\}} = \underset{\boldsymbol{A}_{t-1}}{\mathbb{E}}\left[\boldsymbol{P}_{t-1}^\intercal\boldsymbol{H}_t^{\{t\}}\boldsymbol{P}_{t-1}\right] = diag\{h_{t-1,k}\boldsymbol{I}_{p_k}\}_{k=1}^{K}$, where

$$h_{t-1,k} = \frac{h_{t,k}(K^2+r_{t-1,k}(1-2K))+\sum_{\substack{i=1\\i\neq k}}^{K}h_{t,i}\gamma_{t-1,i}}{K^2}. \quad (81)$$

Repeating until $\boldsymbol{H}_1^{\{t\}} = \underset{\boldsymbol{A}_1}{\mathbb{E}}\left[\boldsymbol{P}_1^\intercal\boldsymbol{H}_2^{\{t\}}\boldsymbol{P}_1\right]$ gives the desired expression in (33). By combining this with (72), we obtain the desired expression for the first term in (78).

We now continue with the second term in (78). With $\boldsymbol{H}_{\tau+1}^{\{t\}} = diag\{h_{\tau+1,k}\boldsymbol{I}_{p_k}\}_{k=1}^{K}$, we apply (70) to write

$$\underset{\boldsymbol{A}_\tau}{\mathbb{E}}\left[\boldsymbol{A}_\tau^\intercal\bar{\boldsymbol{A}}_\tau^\intercal\boldsymbol{H}_{\tau+1}^{\{t\}}\bar{\boldsymbol{A}}_\tau\boldsymbol{A}_\tau\right]$$

$$= diag\left\{\frac{h_{\tau+1}r_{\tau,k}+\sum_{\substack{i=1\\i\neq k}}^{K}h_{\tau+1,i}\gamma_{\tau,i}}{K^2}\boldsymbol{I}_{p_K}\right\}_{k=1}^{K}, \quad (82)$$

and use (69) to write

$$\underset{\boldsymbol{A}_\tau}{\mathbb{E}}\left[\bar{\boldsymbol{A}}_\tau^\intercal\boldsymbol{H}_{\tau+1}^{\{t\}}\bar{\boldsymbol{A}}_\tau\right] = \frac{1}{K^2}\sum_{k=1}^{K}\frac{h_{\tau+1,k}\gamma_{\tau,k}}{n_\tau}\boldsymbol{I}_{n_\tau}. \quad (83)$$

Here, $\boldsymbol{z}_\tau \sim \mathcal{N}(\boldsymbol{0}, \sigma_\tau^2\boldsymbol{I}_{n_\tau})$, hence $\mathbb{E}_{\boldsymbol{z}_\tau}[\|\boldsymbol{z}_\tau\|^2] = n_\tau\sigma_\tau^2$, and

$$\underset{\boldsymbol{z}_\tau}{\mathbb{E}}\left[\|\boldsymbol{z}_\tau\|^2_{\underset{\boldsymbol{A}_\tau}{\mathbb{E}}\left[\bar{\boldsymbol{A}}_\tau^\intercal\boldsymbol{H}_{\tau+1}^{\{t\}}\bar{\boldsymbol{A}}_\tau\right]}\right] = \sigma_\tau^2\frac{\sum_{k=1}^{K}h_{\tau+1,k}\gamma_{\tau,k}}{K^2}. \quad (84)$$

Combining (67) and (68), we find that for $j \geq 1$,

$$\prod_{\ell=j+1}^{\tau-1} \mathbb{E}_{\boldsymbol{A}_\ell}\left[\boldsymbol{P}_\ell\right] \mathbb{E}_{\boldsymbol{A}_j}\left[\bar{\boldsymbol{A}}_j \boldsymbol{A}_j\right]$$

$$= \prod_{\ell=j+1}^{\tau-1} \text{diag}\left\{\left(1-\frac{r_{\ell,k}}{K}\right)\boldsymbol{I}_{p_k}\right\}_{k=1}^{K} \text{diag}\left\{\frac{r_{j,k}}{K}\boldsymbol{I}_{p_k}\right\}_{k=1}^{K} \tag{85}$$

$$= \text{diag}\left\{\frac{r_{j,k}}{K}\prod_{\ell=j+1}^{\tau-1}\left(1-\frac{r_{\ell,k}}{K}\right)\boldsymbol{I}_{p_k}\right\}_{k=1}^{K}, \tag{86}$$

and for $j = 0$,

$$\prod_{\ell=1}^{\tau-1} \mathbb{E}_{\boldsymbol{A}_\ell}\left[\boldsymbol{P}_\ell\right] = \text{diag}\left\{\prod_{\ell=1}^{\tau-1}\left(1-\frac{r_{\ell,k}}{K}\right)\boldsymbol{I}_{p_k}\right\}_{k=1}^{K}. \tag{87}$$

Using (67) and (70), we have that

$$\mathbb{E}_{\boldsymbol{A}_\tau}\left[\boldsymbol{A}_\tau^\intercal \bar{\boldsymbol{A}}_\tau^\intercal \boldsymbol{H}_{\tau+1}^{\{t\}} \boldsymbol{P}_\tau\right]$$

$$= \mathbb{E}_{\boldsymbol{A}_\tau}\left[\boldsymbol{A}_\tau^\intercal \bar{\boldsymbol{A}}_\tau^\intercal \boldsymbol{H}_{\tau+1}^{\{t\}}\right] - \mathbb{E}_{\boldsymbol{A}_\tau}\left[\boldsymbol{A}_\tau^\intercal \bar{\boldsymbol{A}}_\tau^\intercal \boldsymbol{H}_{\tau+1}^{\{t\}} \bar{\boldsymbol{A}}_\tau \boldsymbol{A}_\tau\right] \tag{88}$$

$$= \text{diag}\left\{\frac{h_{\tau+1,k} r_{\tau,k}}{K}\boldsymbol{I}_{p_k}\right\}_{k=1}^{K}$$

$$- \text{diag}\left\{\frac{h_{\tau+1,k} r_{\tau,k} + \sum_{\substack{i=1 \\ i \neq k}}^{K} h_{\tau+1,i}\gamma_{\tau,i}}{K^2}\boldsymbol{I}_{p_k}\right\}_{k=1}^{K}. \tag{89}$$

We now combine (82), (84), (86), (87) and (89), we find the final form of α_τ in (79),

$$\alpha_\tau = \|\boldsymbol{w}_\tau^* - \boldsymbol{w}_i^*\|_{\boldsymbol{R}_\tau^{\{t\}}}^2 + \sigma_\tau^2 \frac{\sum_{k=1}^{K} h_{\tau+1,k}\gamma_{\tau,k}}{K^2}$$

$$+ 2\sum_{j=0}^{\tau-1}\left\langle\boldsymbol{w}_\tau^* - \boldsymbol{w}_i^*, \boldsymbol{w}_j^* - \boldsymbol{w}_i^*\right\rangle_{\boldsymbol{Q}_{\tau,j}^{\{t\}}}, \tag{90}$$

with $\boldsymbol{R}_\tau^{\{t\}}$ and $\boldsymbol{Q}_{\tau,j}^{\{t\}}$ defined as in Theorem 1. Note that we set $\boldsymbol{w}_0^* = \boldsymbol{0}$ and $r_{0,k} = K$ to make the notation more compact. By inserting this expression for α_τ together with the derived expression for $\boldsymbol{H}_1^{\{t\}}$ into (72), we obtain the desired expression in (78), concluding the proof of Theorem 1.

D. Proof of Theorem 2

By inserting $\boldsymbol{w}_t^* = \boldsymbol{w}^*$ and $\sigma_t^2 = \sigma^2$ into $G_T(\hat{\boldsymbol{w}}_T^{(T_c)})$ in (27) and simplifying, the desired expression in (37) is obtained.

We now prove (38) and (39). Recall the definition $\boldsymbol{H}_1^{\{T\}} = \text{diag}\{h_{1,k}\boldsymbol{I}_{p_k}\}_{k=1}^{K}$, with

$$h_{\tau,k} = \frac{h_{\tau+1,k}\left(K^2 + r_{\tau,k}(1-2K)\right) + \sum_{\substack{i=1 \\ i \neq k}}^{K} h_{\tau+1,i}\gamma_{\tau,i}}{K^2}, \tag{91}$$

$\tau = 1, \ldots, T$, and $h_{T+1,k} = 1$, $k = 1, \ldots, K$. Note that $K^2 + r_{\tau,k}(1-2K) \geq 0$ and $\gamma_{\tau,k} > 0$, hence the fraction here is non-negative, and

$$h_{\tau,k} \leq h_{\tau+1,\max} \frac{K^2 - r_{\tau,k}(2K-1) + \sum_{\substack{i=1 \\ i \neq k}}^{K}\gamma_{\tau,i}}{K^2}, \tag{92}$$

where $h_{\tau,\max} = \max_k h_{\tau,k}$. Note that this upper bound is bounded above by replacing $r_{\tau,k}$ with $r_{\tau,\min} = \min_k r_{\tau,k}$ and

$\gamma_{\tau,k}$ with $\gamma_{\tau,\max} = \max_k \gamma_{\tau,k}$, hence

$$h_{\tau,k} \leq h_{\tau+1,\max} \times f_\tau, \tag{93}$$

where

$$f_\tau = \frac{K^2 - (2K-1)r_{\tau,\min} + (K-1)\gamma_{\tau,\max}}{K^2}. \tag{94}$$

We have that

$$h_{1,k} \leq h_{2,\max}f_1 \leq \cdots \leq f_T \cdots f_1, \tag{95}$$

where we have used that $h_{T+1,k} = 1$.

It follows that if $|f_\tau| < 1$, $\forall\tau$, then $\lim_{T\to\infty} h_{1,k} = 0$, and hence $\lim_{T\to\infty} \|\boldsymbol{w}^*\|_{\boldsymbol{H}_1^{\{T\}}}^2 = 0$. We recall that the fraction f_τ is nonnegative and continue by deriving the conditions for which $f_\tau < 1$. We will consider the following two cases separately:

a) $n_\tau < p_k$, $\forall\tau, k$: Here, $r_{\tau,\min} = \frac{n_\tau}{p_{\max}}$ and $\gamma_{\tau,\max} = \frac{n_\tau}{p_{\min} - n_\tau - 1}$. Inserting these identities into $f_\tau < 1$, we obtain

$$\frac{K^2 - (2K-1)\frac{n_\tau}{p_{\max}} + (K-1)\frac{n_\tau}{p_{\min} - n_\tau - 1}}{K^2} < 1. \tag{96}$$

Simplifying this expression gives the condition in (38). Note that the bound in (38) is strictly less than $p_{\min}$, hence the condition $n_\tau < p_k$ of the setting here is included in this bound.

b) $n_\tau > p_k$, $\forall\tau, k$: Here, $r_{\tau,\min} = 1$ and $\gamma_{\tau,\max} = \frac{p_{\min}}{n_\tau - p_{\max} - 1}$. Setting $f_\tau < 1$, we obtain

$$\frac{K^2 - (2K-1) + (K-1)\frac{p_{\min}}{n_\tau - p_{\max} - 1}}{K^2} < 1. \tag{97}$$

Re-arranging this expression gives the bound in (39). Note that the bound in (39) is strictly greater than $p_{\max}$, hence $n_\tau > p_k$ is fulfilled if the bound holds. This concludes the proof.

E. Proof of Lemma 3

Inserting $\boldsymbol{w}_t^* = \boldsymbol{w}^*$ and $\sigma_t^2 = 0$ into $F_T(\hat{\boldsymbol{w}}_T^{(T_c)})$ in (6),

$$F_T(\hat{\boldsymbol{w}}_T^{(T_c)}) = \frac{1}{T}\sum_{i=1}^{T}\frac{1}{2n_i}\mathbb{E}_{\mathcal{D}_T}\left[\left\|\boldsymbol{A}_i(\hat{\boldsymbol{w}}_T^{(T_c)} - \boldsymbol{w}^*)\right\|^2\right]. \tag{98}$$

We apply the submultiplicativity of the ℓ_2-norm,

$$F_T(\hat{\boldsymbol{w}}_T^{(T_c)}) \leq \frac{1}{T}\sum_{i=1}^{T}\frac{1}{2n_i}\mathbb{E}_{\mathcal{D}_T}\left[\|\boldsymbol{A}_i\|^2\left\|\hat{\boldsymbol{w}}_T^{(T_c)} - \boldsymbol{w}^*\right\|^2\right]. \tag{99}$$

For a large number of tasks T, hence for a large number of i.i.d. samples, the estimate $\hat{\boldsymbol{w}}_T^{(T_c)}$ may be assumed to be uncorrelated with $\boldsymbol{A}_i$ [59, Ch. 16]. Hence, we approximate

$$\mathbb{E}_{\mathcal{D}_T}\left[\|\boldsymbol{A}_i\|^2\left\|\hat{\boldsymbol{w}}_T^{(T_c)} - \boldsymbol{w}^*\right\|^2\right] \approx \mathbb{E}_{\boldsymbol{A}_i}\left[\|\boldsymbol{A}_i\|^2\right]\mathbb{E}_{\mathcal{D}_T}\left[\left\|\hat{\boldsymbol{w}}_T^{(T_c)} - \boldsymbol{w}^*\right\|^2\right]. \tag{100}$$

From the proof of Theorem 1, we have (78), which here becomes

$$\mathbb{E}_{\mathcal{D}_T}\left[\left\|\hat{\boldsymbol{w}}_T^{(T_c)} - \boldsymbol{w}^*\right\|^2\right] = \|\boldsymbol{w}^*\|_{\boldsymbol{H}_1^{\{T\}}}^2, \tag{101}$$

where we have used that $\phi(\hat{\boldsymbol{w}}_t^{(T_c)}, \boldsymbol{w}_i^*) = 0$, $\tau = 1, \ldots, T$, because $\boldsymbol{w}_\tau^* = \boldsymbol{w}^*$ and $\sigma_\tau^2 = 0$, see for instance (28). Now if either the condition in (38) or (39) holds for $t = 1, \ldots, T$, then we can apply (40) to (101), to obtain $\lim_{T\to\infty}\mathbb{E}_{\mathcal{D}_T}\left[\left\|\hat{\boldsymbol{w}}_T^{(T_c)} - \boldsymbol{w}^*\right\|^2\right] = 0$. Inserting this into

(100), and (100) into (99), we find that the upper bound in (99) is approximately zero in the limit of $T \to \infty$, i.e., $\lim_{T \to \infty} F_T\left(\hat{\boldsymbol{w}}_T^{(T_c)}\right) \approx 0$. This concludes the proof.

F. Proof of Lemma 5

We first give the following lemma which gives the expression for the last step of the recursion.

Lemma 6. *Let $T_c = 1$ or the partitions of the latest task, task τ, $\boldsymbol{A}_{\tau,[k]}$ be full row rank. Also let the regressors in $\boldsymbol{A}_\tau$ be uncorrelated with the zero-mean noise vector $\boldsymbol{z}_\tau$ and the previous tasks. Then, for any fixed $\boldsymbol{u} \in \mathbb{R}^{p \times 1}$ and some symmetric matrix $\boldsymbol{H} \in \mathbb{R}^{p \times p}$, we have*

$$\mathbb{E}_{\mathcal{D}_\tau}\left[\left\|\hat{\boldsymbol{w}}_\tau^{(T_c)} - \boldsymbol{u}\right\|_{\boldsymbol{H}}^2\right] = \mathbb{E}_{\mathcal{D}_{\tau-1}}\left[\left\|\hat{\boldsymbol{w}}_{\tau-1}^{(T_c)} - \boldsymbol{u}\right\|_{\boldsymbol{H}_\tau}^2\right] + \alpha_\tau, \quad (102)$$

where $\boldsymbol{H}_\tau = \mathbb{E}_{\boldsymbol{A}_\tau}\left[\boldsymbol{P}_\tau^\mathsf{T} \boldsymbol{H} \boldsymbol{P}_\tau\right]$ and

$$\alpha_\tau = \|\boldsymbol{w}_\tau^* - \boldsymbol{u}\|_{\mathbb{E}_{\boldsymbol{A}_\tau}[\boldsymbol{A}_\tau^\mathsf{T} \bar{\boldsymbol{A}}_\tau^\mathsf{T} \boldsymbol{H} \bar{\boldsymbol{A}}_\tau \boldsymbol{A}_\tau]}^2 + \mathbb{E}_{\boldsymbol{z}_\tau}\left[\|\boldsymbol{z}_\tau\|_{\mathbb{E}_{\boldsymbol{A}_\tau}[\bar{\boldsymbol{A}}_\tau^\mathsf{T} \boldsymbol{H} \bar{\boldsymbol{A}}_\tau]}^2\right]$$

$$+ 2\left\langle \boldsymbol{w}_\tau^* - \boldsymbol{u}, \mathbb{E}_{\mathcal{D}_{\tau-1}}\left[\hat{\boldsymbol{w}}_{\tau-1}^{(T_c)} - \boldsymbol{u}\right]\right\rangle_{\mathbb{E}_{\boldsymbol{A}_\tau}[\boldsymbol{A}_\tau^\mathsf{T} \bar{\boldsymbol{A}}_\tau^\mathsf{T} \boldsymbol{H} \boldsymbol{P}_\tau]}. \quad (103)$$

Proof: See Appendix G.

We will now use (102) on $\mathbb{E}_{\mathcal{D}_t}\left[\left\|\hat{\boldsymbol{w}}_t^{(T_c)} - \boldsymbol{u}\right\|^2\right]$ recursively. Starting with $\boldsymbol{H} = \boldsymbol{I}_p$, we write

$$\mathbb{E}_{\mathcal{D}_t}\left[\left\|\hat{\boldsymbol{w}}_t^{(T_c)} - \boldsymbol{u}\right\|^2\right] = \mathbb{E}_{\mathcal{D}_{t-1}}\left[\left\|\hat{\boldsymbol{w}}_{t-1}^{(T_c)} - \boldsymbol{u}\right\|_{\mathbb{E}_{\mathcal{D}_t}[\boldsymbol{P}_t^\mathsf{T} \boldsymbol{P}_t]}^2\right] + \alpha_t$$

$$= \mathbb{E}_{\mathcal{D}_{t-2}}\left[\left\|\hat{\boldsymbol{w}}_{t-2}^{(T_c)} - \boldsymbol{u}\right\|_{\mathbb{E}_{\mathcal{D}_t}[\boldsymbol{P}_{t-1}^\mathsf{T} \boldsymbol{P}_t^\mathsf{T} \boldsymbol{P}_t \boldsymbol{P}_{t-1}]}^2\right] + \alpha_t + \alpha_{t-1} \quad (104)$$

$$= \cdots = \|\boldsymbol{u}\|_{\boldsymbol{H}_1^{\{t\}}}^2 + \sum_{\tau=1}^t \alpha_\tau, \quad (105)$$

where $\boldsymbol{H}_1^{\{t\}} = \mathbb{E}_{\mathcal{D}_t}\left[\boldsymbol{P}_1^\mathsf{T} \cdots \boldsymbol{P}_t^\mathsf{T} \boldsymbol{P}_t \cdots \boldsymbol{P}_1\right]$ and we have used that we initialize the continual learning procedure with $\boldsymbol{w}_0 = \boldsymbol{0}$.

Lemma 7. *Within the setting of Lemma 5, the following holds,*

$$\mathbb{E}_{\mathcal{D}_{\tau-1}}\left[\hat{\boldsymbol{w}}_{\tau-1}^{(T_c)} - \boldsymbol{u}\right] = \sum_{j=0}^{\tau-1}\left(\prod_{\ell=j+1}^{\tau-1}\left(\mathbb{E}_{\boldsymbol{A}_\ell}[\boldsymbol{P}_\ell]\right)\mathbb{E}_{\boldsymbol{A}_j, \boldsymbol{z}_j}[\boldsymbol{s}_j]\right), \quad (106)$$

where $\boldsymbol{s}_0 = -\boldsymbol{u}$ and $\boldsymbol{s}_j = \bar{\boldsymbol{A}}_j \boldsymbol{A}_j(\boldsymbol{w}_j^* - \boldsymbol{u}) + \bar{\boldsymbol{A}}_j \boldsymbol{z}_j$, $j = 1, \ldots, \tau - 1$.

Proof: See Appendix H.

Inserting the result of Lemma 7 into (103) and combining with (105), the desired expression for α_τ is obtained.

G. Proof of Lemma 6

Using the recursion in (23), and the notation $\boldsymbol{w}_\tau = \hat{\boldsymbol{w}}_\tau^{(T_c)}$ and $\boldsymbol{w}_{\tau-1} = \hat{\boldsymbol{w}}_{\tau-1}^{(T_c)}$, we can write

$$\|\boldsymbol{w}_\tau - \boldsymbol{u}\|_{\boldsymbol{H}}^2 = \|\boldsymbol{P}_\tau(\boldsymbol{w}_{\tau-1} - \boldsymbol{u})\|_{\boldsymbol{H}}^2 + \|\bar{\boldsymbol{A}}_\tau \boldsymbol{A}_\tau(\boldsymbol{w}_\tau^* - \boldsymbol{u})\|_{\boldsymbol{H}}^2$$

$$+ \|\bar{\boldsymbol{A}}_\tau \boldsymbol{z}_\tau\|_{\boldsymbol{H}}^2 + 2\left\langle \bar{\boldsymbol{A}}_\tau \boldsymbol{A}_\tau(\boldsymbol{w}_\tau^* - \boldsymbol{u}), \boldsymbol{P}_\tau(\boldsymbol{w}_{\tau-1} - \boldsymbol{u})\right\rangle_{\boldsymbol{H}}$$

$$+ 2\left\langle \boldsymbol{P}_\tau(\boldsymbol{w}_{\tau-1} - \boldsymbol{u}) + \bar{\boldsymbol{A}}_\tau \boldsymbol{A}_\tau(\boldsymbol{w}_\tau^* - \boldsymbol{u}), \bar{\boldsymbol{A}}_\tau \boldsymbol{z}_\tau\right\rangle_{\boldsymbol{H}} \quad (107)$$

Since $\boldsymbol{H}$ is fixed, hence independent from the random entities, the expectation w.r.t. $\mathcal{D}_\tau$ of the final term is zero, because

$\boldsymbol{z}_\tau$ is zero-mean and uncorrelated with $\boldsymbol{w}_{\tau-1}$ and $\boldsymbol{A}_\tau$, hence also with $\boldsymbol{P}_\tau$. For the other terms, the desired expression is obtained by using the uncorrelatedness between $\boldsymbol{w}_{\tau-1}$ and $\boldsymbol{A}_\tau$, and between $\boldsymbol{z}_\tau$ and $\boldsymbol{A}_\tau$. We here illustrate the derivation of the first term,

$$\mathbb{E}_{\mathcal{D}_\tau}\left[\|\boldsymbol{P}_\tau(\boldsymbol{w}_{\tau-1} - \boldsymbol{u})\|_{\boldsymbol{H}}^2\right]$$
$$= \mathbb{E}_{\mathcal{D}_{\tau-1}}\left[(\boldsymbol{w}_{\tau-1} - \boldsymbol{u})^\mathsf{T} \mathbb{E}_{\boldsymbol{A}_\tau}\left[\boldsymbol{P}_\tau^\mathsf{T} \boldsymbol{H} \boldsymbol{P}_\tau\right](\boldsymbol{w}_{\tau-1} - \boldsymbol{u})\right]$$
$$= \mathbb{E}_{\mathcal{D}_{\tau-1}}\left[\|\boldsymbol{w}_{\tau-1} - \boldsymbol{u}\|_{\mathbb{E}_{\boldsymbol{A}_\tau}[\boldsymbol{P}_\tau^\mathsf{T} \boldsymbol{H} \boldsymbol{P}_\tau]}^2\right].$$

The remaining terms are found in a similar fashion.

H. Proof of Lemma 7

Here, we use the notation notation $\boldsymbol{w}_j = \hat{\boldsymbol{w}}_j^{(T_c)}$, for $j = 0, \ldots, \tau - 1$. Since the recursion in (23) holds for the tasks $1, \ldots, t-1$, we have

$$\boldsymbol{w}_{\tau-1} - \boldsymbol{u} = \boldsymbol{P}_{\tau-1}(\boldsymbol{w}_{\tau-2} - \boldsymbol{u}) + \boldsymbol{s}_{\tau-1} \quad (108)$$

$$= \boldsymbol{P}_{\tau-1}(\boldsymbol{P}_{\tau-2}(\boldsymbol{w}_{\tau-3} - \boldsymbol{u}) + \boldsymbol{s}_{\tau-2}) + \boldsymbol{s}_{\tau-1} \quad (109)$$

$$= \boldsymbol{P}_{\tau-1} \cdots \boldsymbol{P}_1(\boldsymbol{w}_0 - \boldsymbol{u})$$
$$+ \boldsymbol{P}_{\tau-1} \cdots \boldsymbol{P}_2 \boldsymbol{s}_1 + \cdots + \boldsymbol{P}_{\tau-1} \boldsymbol{s}_{\tau-2} + \boldsymbol{s}_{\tau-1} \quad (110)$$

$$= \sum_{j=0}^{\tau-1}\left(\prod_{\ell=j+1}^{\tau-1} \boldsymbol{P}_\ell\right) \boldsymbol{s}_j, \quad (111)$$

where $\boldsymbol{s}_0 = -\boldsymbol{u}$. The matrices $\boldsymbol{A}_\ell$, $\ell = 1, \ldots, t-1$ are all uncorrelated with each other and with $\boldsymbol{z}_\ell$, thus taking the expectation w.r.t. $\mathcal{D}_{\tau-1}$ gives the desired expression.

REFERENCES

[1] G. I. Parisi, R. Kemker, J. L. Part, C. Kanan *et al.*, "Continual lifelong learning with neural networks: A review," *Neural Networks*, vol. 113, pp. 54–71, 2019.

[2] J. Kirkpatrick, R. Pascanu, N. Rabinowitz, J. Veness *et al.*, "Overcoming catastrophic forgetting in neural networks," *Proc. of the National Academy of Sciences*, vol. 114, no. 13, pp. 3521–3526, mar 2017.

[3] M. De Lange, R. Aljundi, M. Masana, S. Parisot *et al.*, "A continual learning survey: Defying forgetting in classification tasks," *IEEE Trans. Pattern Anal. Mach. Intell.*, vol. 44, no. 7, pp. 3366–3385, 2022.

[4] H. Sun, W. Pu, X. Fu, T.-H. Chang *et al.*, "Learning to continuously optimize wireless resource in a dynamic environment: A bilevel optimization perspective," *IEEE Trans. on Signal Process.*, vol. 70, pp. 1900–1917, 2022.

[5] I. Evron, E. Moroshko, R. Ward, N. Srebro *et al.*, "How catastrophic can catastrophic forgetting be in linear regression?" in *Proc. of Thirty Fifth Conf. on Learning Theory*. PMLR, Jul 2022, pp. 4028–4079.

[6] R. M. French, "Catastrophic forgetting in connectionist networks," *Trends in Cognitive Sciences*, vol. 3, no. 4, pp. 128–135, 1999.

[7] T. Doan, M. Abbana Bennani, B. Mazoure, G. Rabusseau *et al.*, "A theoretical analysis of catastrophic forgetting through the NTK overlap matrix," in *Proc. of The 24th Inter. Conf. on Artif. Intell. and Stat.*, 2021.

[8] M. A. Bennani, T. Doan, and M. Sugiyama, "Generalisation guarantees for continual learning with orthogonal gradient descent," *arxiv:2006.11942*, Dec. 2020.

[9] A. Sayed, *Adaptive Filters*, ser. IEEE Press. Wiley, 2008.

[10] H. Nosrati, M. Shamsi, S. M. Taheri, and M. H. Sedaaghi, "Adaptive networks under non-stationary conditions: Formulation, performance analysis, and application," *IEEE Trans. on Signal Process.*, vol. 63, pp. 4300–4314, 2015.

[11] E. Fox, E. B. Sudderth, M. I. Jordan, and A. S. Willsky, "Bayesian nonparametric inference of switching dynamic linear models," *IEEE Trans. on Signal Process.*, vol. 59, no. 4, pp. 1569–1585, 2011.

[12] J. Ding, S. Shahrampour, K. Heal, and V. Tarokh, "Analysis of multistate autoregressive models," *IEEE Trans. on Signal Process.*, vol. 66, 2018.

[13] P. Karimi, M. D. Butala, Z. Zhao, and F. Kamalabadi, "Efficient model selection in switching linear dynamic systems by graph clustering," *IEEE Signal Process. Letters*, vol. 29, pp. 2482–2486, 2022.

[14] I. J. Goodfellow, M. Mirza, D. Xiao, A. Courville *et al.*, "An empirical investigation of catastrophic forgetting in gradient-based neural networks," *arxiv:1312.6211*, Mar. 2015.

[15] C. V. Nguyen, A. Achille, M. Lam, T. Hassner *et al.*, "Toward understanding catastrophic forgetting in continual learning," *arxiv:1908.01091*, Aug. 2019.

[16] S. Farquhar and Y. Gal, "Towards robust evaluations of continual learning," *arxiv:1805.09733*, Jun. 2019.

[17] V. V. Ramasesh, E. Dyer, and M. Raghu, "Anatomy of catastrophic forgetting: Hidden representations and task semantics," *Inter. Conf. on Learning Representations*, May 2021.

[18] S. Lin, P. Ju, Y. Liang, and N. Shroff, "Theory on forgetting and generalization of continual learning," in *Proc. of the 40th Inter. Conf. on Machine Learning*, ser. Proceedings of Machine Learning Research, vol. 202. PMLR, 23–29 Jul 2023.

[19] S. Wang, T. Tuor, T. Salonidis, K. K. Leung *et al.*, "Adaptive federated learning in resource constrained edge computing systems," *IEEE J. Sel. Areas Commun.*, vol. 37, no. 6, pp. 1205–1221, 2019.

[20] S. Niknam, H. S. Dhillon, and J. H. Reed, "Federated learning for wireless communications: Motivation, opportunities, and challenges," *IEEE Commun. Mag.*, vol. 58, no. 6, pp. 46–51, 2020.

[21] X. Wang, H. Ishii, L. Du, P. Cheng *et al.*, "Privacy-preserving distributed machine learning via local randomization and ADMM perturbation," *IEEE Trans. Signal Process.*, vol. 68, pp. 4226–4241, 2020.

[22] M. Rabbat and R. Nowak, "Distributed optimization in sensor networks," *Proc. 3rd Int. Symp. on Inf. Proc. in Sensor Netw.*, pp. 20–27, 2004.

[23] S. Kar and J. M. F. Moura, "Distributed consensus algorithms in sensor networks with imperfect communication: Link failures and channel noise," *IEEE Trans. on Signal Process.*, vol. 57, pp. 355–369, 2009.

[24] F. Hua, R. Nassif, C. Richard, H. Wang *et al.*, "Diffusion LMS with communication delays: Stability and performance analysis," *IEEE Signal Process. Letters*, vol. 27, pp. 730–734, 2020.

[25] A. H. Sayed, "Adaptation, learning, and optimization over networks," *Foundations and Trends in Machine Learning*, vol. 7, pp. 311–801, 2014.

[26] J. Chen, Z. J. Towfic, and A. H. Sayed, "Dictionary learning over distributed models," *IEEE Trans. on Signal Process.*, vol. 63, no. 4, pp. 1001–1016, 2015.

[27] V. Smith, S. Forte, C. Ma, M. Takáč *et al.*, "CoCoA: A general framework for communication-efficient distributed optimization," *J. Mach. Learn. Res.*, vol. 18, no. 1, pp. 8590–8638, 2017.

[28] M. Jaggi, V. Smith, M. Takác, J. Terhorst *et al.*, "Communication-efficient distributed dual coordinate ascent," *Adv. Neural Inf. Process. Systems*, pp. 3068–3076, 2014.

[29] C. Ma, J. Konečnỳ, M. Jaggi, V. Smith *et al.*, "Distributed optimization with arbitrary local solvers," *Optimization Methods and Softw.*, vol. 32, no. 4, pp. 813–848, 2017.

[30] L. He, A. Bian, and M. Jaggi, "Cola: Decentralized linear learning," *Adv. Neural Inf. Process. Syst.*, pp. 4536–4546, 2018.

[31] J. Tsitsiklis, D. Bertsekas, and M. Athans, "Distributed asynchronous deterministic and stochastic gradient optimization algorithms," *IEEE Trans. Automat. Control*, vol. 31, no. 9, pp. 803–812, 1986.

[32] U. A. Khan and J. M. F. Moura, "Distributing the Kalman filter for large-scale systems," *IEEE Trans. Signal Process.*, vol. 56, no. 10, pp. 4919–4935, 2008.

[33] Y. Ye, M. Xiao, and M. Skoglund, "Randomized neural networks based decentralized multi-task learning via hybrid multi-block ADMM," *IEEE Trans. on Signal Process.*, vol. 69, pp. 2844–2857, 2021.

[34] J. Chen, C. Richard, and A. H. Sayed, "Multitask diffusion adaptation over networks," *IEEE Trans. on Signal Process.*, vol. 62, no. 16, pp. 4129–4144, 2014.

[35] R. Nassif, S. Vlaski, C. Richard, J. Chen *et al.*, "Multitask learning over graphs: An approach for distributed, streaming machine learning," *IEEE Signal Process. Magazine*, vol. 37, no. 3, pp. 14–25, 2020.

[36] J. Yoon, W. Jeong, G. Lee, E. Yang *et al.*, "Federated Continual Learning with Weighted Inter-client Transfer," in *Proceedings of the 38 th International Conference on Machine Learning (PLMR)*, 2021.

[37] J. Dong, L. Wang, Z. Fang, G. Sun *et al.*, "Federated Class-Incremental Learning," in *2022 IEEE/CVF Conference on Computer Vision and Pattern Recognition (CVPR)*, Jun. 2022, pp. 10 154–10 163.

[38] D. Shenaj, M. Toldo, A. Rigon, and P. Zanuttigh, "Asynchronous Federated Continual Learning," in *IEEE/CVF Conf. on Computer Vision and Pattern Recognition Workshops (CVPRW)*, 2023, pp. 5055–5063.

[39] M. Hellkvist, A. Özçelikkale, and A. Ahlén, "Continual learning with distributed optimization: Does CoCoA forget?" *arXiv:2211.16994*, 2022.

[40] M. Hellkvist, A. Özçelikkale, and A. Ahlén, "Linear regression with distributed learning: A generalization error perspective," *IEEE Trans. on Signal Process.*, vol. 69, pp. 5479–5495, 2021.

[41] G. M. van de Ven and A. S. Tolias, "Three scenarios for continual learning," *arxiv:1904.07734*, 2019.

[42] C. Zhang, S. Bengio, M. Hardt, B. Recht *et al.*, "Understanding deep learning requires rethinking generalization," in *Inter. Conf. on Learning Representations*, 2017.

[43] B. Song, I. Tsaknakis, C.-Y. Yau, H.-T. Wai *et al.*, "Distributed Optimization for Overparameterized Problems: Achieving Optimal Dimension Independent Communication Complexity," in *Advances in Neural Information Processing Systems*, 2022.

[44] P. Khanduri, H. Yang, M. Hong, J. Liu *et al.*, "Decentralized learning for overparameterized problems: A multi-agent kernel approximaiton approach," in *Inter. Conf. on Learning Representations*, 2022.

[45] C. Zhang and Q. Li, "Distributed Optimization for Over-Parameterized Learning," *arXiv:1906.06205*, Jun. 2019.

[46] T. Qin, S. R. Etesami, and C. A. Uribe, "Decentralized Federated Learning for Over-Parameterized Models," in *IEEE 61st Conference on Decision and Control (CDC)*, Dec. 2022, pp. 5200–5205.

[47] Y. Deng, M. M. Kamani, and M. Mahdavi, "Local SGD Optimizes Overparameterized Neural Networks in Polynomial Time," in *Inter. Conf. on Artificial Intelligence and Statistics*, 2022.

[48] P. Nakkiran, P. Venkat, S. M. Kakade, and T. Ma, "Optimal regularization can mitigate double descent," in *Int. Conf. Learning Representations*, 2021.

[49] T. Hastie, A. Montanari, S. Rosset, and R. J. Tibshirani, "Surprises in high-dimensional ridgeless least squares interpolation," *arXiv:1903.08560*, 2020.

[50] V. Muthukumar, K. Vodrahalli, V. Subramanian, and A. Sahai, "Harmless interpolation of noisy data in regression," *IEEE J. on Sel. Areas in Inf. Theory*, vol. 1, no. 1, pp. 67–83, 2020.

[51] S. U. Stich, "Local SGD Converges Fast and Communicates Little," in *Inter. Conf. on Learning Representations*, 2019.

[52] S. Salehkaleybar, A. Sharifnassab, and S. J. Golestani, "One-Shot Federated Learning: Theoretical Limits and Algorithms to Achieve Them," *J. Mach. Learn. Res.*, vol. 22, Jan 2021.

[53] A. Sharifnassab, S. Salehkaleybar, and S. J. Golestani, "Order Optimal One-Shot Distributed Learning," in *Advances in Neural Information Processing Systems*, 2019.

[54] C. Heinze, B. McWilliams, N. Meinshausen, and G. Krummenacher, "LOCO: Distributing Ridge Regression with Random Projections," *arXiv:1406.3469*, Jun. 2015.

[55] C. Heinze, B. McWilliams, and N. Meinshausen, "DUAL-LOCO: Distributing statistical estimation using random projections," in *Proc. of the 19th Inter. Conf. on Artificial Intelligence and Statistics*, vol. 51, May 2016, pp. 875–883.

[56] G. Mann, R. Mcdonald, M. Mohri, N. Silberman *et al.*, "Efficient large-scale distributed training of conditional maximum entropy models," in *Advances in Neural Information Processing Systems*, vol. 22, 2009.

[57] Y. Zhang, J. C. Duchi, and M. J. Wainwright, "Communication-efficient algorithms for statistical optimization," *J. Mach. Learn. Res.*, vol. 14, p. 3321–3363, 2013.

[58] A. Spiridonoff, A. Olshevsky, and I. Paschalidis, "Communication-efficient SGD: From local SGD to one-shot averaging," in *Advances in Neural Information Processing Systems*, 2021.

[59] S. Haykin, *Adaptive Filter Theory*. Prentice-Hall, Inc., 1996.

[60] Y. LeCun, C. Cortes, and C. J. C. Burges, "MNIST handwritten digit database," 2010. [Online]. Available: http://yann.lecun.com/exdb/mnist/

[61] F. Zenke, B. Poole, and S. Ganguli, "Continual learning through synaptic intelligence," in *Proc. of the 34th Inter. Conf. on Machine Learning - Volume 70*, 2017, p. 3987–3995.

[62] A. Rahimi and B. Recht, "Random features for large-scale kernel machines," *Adv. Neural Inf. Process. Syst.*, pp. 1177–1184, 2008.

[63] C. Bishop, *Pattern Recognition and Machine Learning*, ser. Information Science and Statistics. Springer, 2006.

[64] M. Hellkvist, A. Özçelikkale, and A. Ahlén, "Estimation under model misspecification with fake features," *IEEE Trans. on Signal Process.*, vol. 71, pp. 47–60, 2023.

[65] R. D. Cook and L. Forzani, "On the mean and variance of the generalized inverse of a singular Wishart matrix," *Electron. J. Statist.*, vol. 5, pp. 146–158, 2011.